Zoological Studies **63**:34 (2024)
doi:10.6620/ZS.2024.63-34

Zoological Studies

Open Access

Taxonomic Study of the Chalcidoid Wasps *Sycoscapter* Saunders (Hymenoptera: Pteromalidae) Associated with Monoecious *Ficus* in Taiwan, with Description of Four New Species

Po-An Chou[1], Wen-Bin Yeh[2], Zhi-Hui Su[3], and Hsy-Yu Tzeng[1,*]

[1]*Department of Forestry, National Chung Hsing University, No. 145 Xinda Rd., Taichung City 40227, Taiwan.*
**Correspondence: E-mail: erecta@nchu.edu.tw (Tzeng), Fax: +86 04 2287 3628*
E-mail: hut23939889@gmail.com (Chou)
[2]*Department of Entomology, National Chung Hsing University, No. 145 Xinda Rd., Taichung City 40227, Taiwan. E-mail: wbyeh@nchu.edu.tw (Yeh)*
[3]*JT Biohistory Research Hall, Takatsuki, Osaka 569-1125, Japan. E-mail: su.zhihui@brh.co.jp (Su)*

urn:lsid:zoobank.org:pub:1F1AF040-147B-4A45-A475-C8F6EB263DE1
Received 2 February 2024 / Accepted 26 June 2024 / Published 25 December 2024
Communicated by Y. Miles Zhang

As a prominent group of nonpollinating fig wasps widely distributed in the paleotropics, *Sycoscapter* Saunders has been subject to limited taxonomic attention. This study presents the first comprehensive taxonomic investigation of *Sycoscapter* wasps associated with five Taiwanese monoecious fig species, employing both molecular and morphological methods. Phylogenetic analyses using *COI* and *COI+28S* data revealed the presence of five species associated with monoecious figs in Taiwan and neighboring regions: *Sycoscapter gajimaru* (Ishii), *Sycoscapter piceoscapus* Chou & Tzeng sp. nov., *Sycoscapter monticola* Chou & Tzeng sp. nov., *Sycoscapter ishiianus* Chou & Tzeng sp. nov., and *Sycoscapter littoralis* Chou & Tzeng sp. nov. Morphologically, these five *Sycoscapter* species possessed distinctive characteristics, including the male head shape, which distinguished them from related species. Furthermore, males of all five species exhibited rudimentary wing vestiges, commonly found in wasps associated with monoecious figs but absent in those associated with dioecious figs. Overall, this study enriches our understanding of chalcidoid fauna in Taiwan and provides insight into the mechanisms that sustain intricate ecosystems.

Key words: Fig wasp, Sycoryctinae, Sycoryctini, Rudimentary wing, Symbiosis

BACKGROUND

The obligate symbiosis between fig trees (*Ficus* L.) and chalcidoid wasps (Hymenoptera), especially Agaonidae and Pteromalidae, serves as a well-established model for exploring speciation and coevolution (Weiblen 2002; Borges 2015). In this context, the subtribe Sycoryctina (http://www.figweb.org; van Noort and Rasplus 2024) of Otitesellini in Pteromalidae is one of the most common groups interacting with figs and agaonid wasps in the paleotropics (Segar et al. 2012; Burks et al. 2022). Since female Sycoryctina wasps, as external exploiters, use their elongated ovipositors to extract resources from within figs for their offspring, the lengths of ovipositors must correspond to the fig-wall thicknesses (Tzeng et al. 2014). Consequently, they exhibit high host-specific speciation and contribute substantially to the tribe's diversity (McLeish et al. 2010).

The genus *Sycoscapter* Saunders, one of the most diverse group of Sycoryctina, comprises 23 described species from Africa and Asia (Bouček 1988;

Citation: Chou PA, Yeh WB, Su ZH, Tzeng HY. 2024. Taxonomic study of the chalcidoid wasps *Sycoscapter* Saunders (Hymenoptera: Pteromalidae) associated with monoecious *Ficus* in Taiwan, with description of four new species. Zool Stud **63**:34. doi:10.6620/ZS.2024.63-34.

Berg and Wiebes 1992; Segar et al. 2012). However, differentiating *Sycoscapter* from other genera within the same tribe has been complicated by changeable diagnostic characters. Consequently, Bouček (1988) suggested the concept of consolidating all genera into *Sycoscapter s.l.* to resolve this ambiguity in Sycoryctini. Nevertheless, advancements in morphological analyses and molecular phylogeny have brought about the possibility of establishing a natural taxonomic system for Sycoryctini (Berg and Wiebes 1992; Segar et al. 2012). Presently, the genera synonymized by Bouček (1988) are reinstated and the diagnostic criteria for *Sycoscapter s.s.* encompass the following: in females, the forewing features a "boot-like" stigma and robust hairs, with symmetric funicular segments; in males, mesonotum is fused with metanotum and propodeum, and the basitarsus of the hind leg remains unexpanded (Berg and Wiebes 1992; Segar et al. 2012; Pramanik and Dey 2019).

As a vital component of fig-wasp symbiosis, including interactions involving *Sycoscapter*, fig trees are key elements of tropical and subtropical ecosystems, encompassing approximately 750 described species (Berg and Corner 2005). Depending on the flower types in figs, *Ficus* species can be categorized as monoecious or functionally dioecious, with approximately half of all species falling into each category (Berg and Corner 2005; Cruaud et al. 2012; Gardner et al. 2023). Monoecious figs possess protogynous female and male flowers in each fig. Consequently, female flowers develop galls when oviposited, whereas the remainder form seeds through pollen transferred by the wasps. In contrast, functional dioecious figs allocate female flowers to distinct figs, with female figs containing fertile female flowers and male figs possessing male and infertile female flowers, which only form galls. Agaonid wasps associated with functional dioecious figs can lay eggs in the infertile female flowers of male figs but facilitate pollination in female figs without leaving offspring (Weiblen 2002). The coexistence of all flower types in a monoecious fig creates mixed layers of developing seeds and galls, promoting diverse and complex fig-wasp communities (Kerdelhué and Rasplus 1996). Moreover, as an increasing number of studies report the involvement of cryptic species in shaping these intricate fig-wasp communities in monoecious figs (Cook and Bean 2006; Darwell and Cook 2017), the necessity for comprehensive taxonomic studies employing phylogenetic analyses and species delineation becomes evident, with the specific aim of elucidating the functioning of this intricate ecosystem.

In recent decades, researches on *Sycoscapter* wasps have predominantly focused on ecological and evolutionary aspects (McLeish et al. 2010 2012; Sutton et al. 2016), with taxonomic studies remaining relatively scarce (Bouček 1988; Berg and Wiebes 1992; Pramanik and Dey 2019). In Taiwan, fig trees play an important ecological role in lowland vegetation, with some monoecious species being representative plants in urban environments (Chao et al. 2008; Walther et al. 2018). However, similar to the limited taxonomic research on symbiotic *Sycoscapter* wasps globally, only a few species have been documented in Taiwan, as noted by Chen et al. (1999). Therefore, using both morphological and phylogenetic approaches, the present study comprises a comprehensive taxonomic investigation of *Sycoscapter* wasps associated with Taiwanese monoecious fig species. The study aims to provide insight into the delimitation of cryptic species and enhance our understanding of the symbiotic relationship between figs and *Sycoscapter* wasps.

MATERIALS AND METHODS

Among the 28 Taiwanese *Ficus* taxa, 6 are monoecious species. These include *Ficus nervosa* Heyne ex Roth, *Ficus pubinervis* Bl., *Ficus benjamina* L. var. *bracteata* Corner, *Ficus caulocarpa* (Miq.) Miq., *Ficus microcarpa* L. f., and *Ficus subpisocarpa* Gagnep. Notably, the former two species belong to the subgenus *Pharmacosycea*, whereas the remaining four belong to the subgenus *Spherosuke* (Berg 2005 and Corner; Gardner et al. 2023). With the exception of *F. pubinervis*, which approaches its northern distribution boundary on Lanyu and Ludao islands, the other monoecious fig species exhibit broad distribution encompassing not only the whole of Taiwan but also extending to regions in South China and the Ryukyu islands of Japan (Table S1).

Given their wide distribution, D-phase figs (those ready for wasp release) were collected from various locations in Taiwan. Additionally, samples of *F. microcarpa* from adjacent regions were included in this study. Upon collection, figs were placed in containers with fine mesh until wasps emerged. Subsequently, all wasps were preliminarily identified and preserved in 95% alcohol. In addition, related specimens were also examined from museums and institutes, including the following: Department of Entomology at National Chung Hsing University, Taichung, Taiwan (NCHU); Taiwan Agricultural Research Institute, Taichung, Taiwan (TARI); Institute for Agro-Environmental Sciences, Ibaraki, Japan (NARO); and the Chinese Academy of Sciences, China (CAS).

For each population, one to five adult wasps were randomly selected, and genomic DNA was extracted from the whole body using the QuickExtract DNA

Extraction Kit (Epicentre Biotechnologies, Madison, WI). Tissue was ground in 50 µL of QuickExtract solution and incubated at 65°C for 15 min, followed by 98°C for 2 min. A mitochondrial DNA gene, *COI*, and a nuclear ribosomal DNA gene, *28S*, were used for molecular analyses of *Sycoscapter* wasps. Besides, combined *COI+28S* molecular data are recognized as valuable and commonly used in fig-wasp studies (Lopez-Vaamonde et al. 2009; Azuma et al. 2010; Yang et al. 2014). Primer sets LCO1490/HCO2198 for *COI* and D2-3551F/D2—4068R for *28S* were used to amplify the two respective genes. Polymerase chain reaction conditions for the primer sets followed those described by Cruaud et al. (2010) and Heraty et al. (2004). After amplification, products were sequenced from both ends using a Taq Dye Terminator Cycle Sequencing Kit and an ABI 377A sequencer. All sequences have been deposited in GenBank under the following accession numbers: PP111396—PP111462 for *COI* sequences and PP162908—PP162951 for *28S* sequences. Additionally, *COI* sequences of related wasp species from GenBank were incorporated into this study, including three populations of *Sycoscapter* associated with *F. benjamina* L., *F. microcarpa* L. f. and *F. nervosa* B. Heyne ex Roth.

Sequence alignment of *COI* was performed using the ClustalW algorithm in MEGA 11 (Tamura et al. 2021), and that of *28S* was conducted on TurboFold II web server (https://rna.urmc.rochester.edu/RNAstructureWeb/Servers/TurboFold.html; Tan et al. 2017). Two fig wasp species, *Walkerella kurandensis* ex *F. microcarpa* (Pteromalidae: Otitesellini: Otitesellina) and *Sycoryctes patellais* ex *Ficus variegata* (Pteromalidae: Otitesellini: Sycoryctina), belonging to the same tribe as *Sycoscapter* (http://www.figweb.org; van Noort and Rasplus 2024) were chosen as outgroup species. Owing to the unavailability of *28S* sequences for the related species in GenBank, we constructed *28S* tree and *COI+28S* tree based on the sequences generated in this study. Nucleotide substitution models GTR+I+G and GTR+I were determined as the best-fitting models for the *COI* gene and the *28S* gene, respectively, using PartitionFinder 2 (Lanfear et al. 2012). Phylogenetic analyses were conducted using the maximum likelihood (ML) method on the IQ-TREE web server (http://iqtree.cibiv.univie.ac.at/) employing 1,000 ultrafast bootstrap replications (Nguyen et al. 2015; Trifinopoulos et al. 2016; Hoang et al. 2018). Bayesian inference (BI) analyses were conducted using MrBayes 3.2.7 (Ronquist et al. 2012), running Markov chain Monte Carlo methods for fifty million generations with sampling every 100 generations. Convergence was determined using Tracer 1.7.2 (Rambaut et al. 2018) with a threshold of all ESS parameters >200, and the initial 10% of trees were discarded as the burn-in. To determine the species delimitation of these *Sycoscapter* wasps in Taiwan, pairwise nucleotide divergence with Kimura 2-parameter (K2P) distance of *COI* gene and PTP model were conducted with MEGA 11 (Tamura et al. 2021) and bPTP web server (https://species.h-its.org/) employing 100,000 MCMC generations (Zhang et al. 2013), respectively.

Morphological measurements were performed using specimen and scanning electron microscopy (SEM) images captured with Keyence VHX and Hitachi S3400N microscopes, respectively. To prepare specimens for imaging, wasps were subjected to 1 min of agitation in an ultrasonic cleaner to remove pollen. Subsequently, specimens were serially dehydrated using ethanol and hexamethyldisilazane (Heraty and Hawks 1998) or critical point drying methods (Quoram E3100). Following dehydration, wasps were dissected and mounted on cards for specimen imaging or dissected and coated with gold using a Quorum SC7620 for SEM imaging. ImageJ software was used to perform measurements. The morphological terminology used in this study followed Bouček and Rasplus (1991) and Berg and Wiebes (1992). To assess the morphological relationship between *Sycoscapter* wasps associated with Taiwanese monoecious figs and similar described species, we followed the key provided by Priyadasarnan (2000) and Pramanik and Dey (2019), subsequently creating comparison tables. Abbreviations used in the taxonomic description include the following: L: length; W: width; H: height; POL: postocellar distance; and OOL: ocellocular distance.

RESULTS

Among the six monoecious fig tree species in Taiwan, *F. pubinervis* was notable for its absence of *Sycoscapter* wasps. Conversely, all other species exhibited a high prevalence and abundance of *Sycoscapter* wasps within their figs. In total, 81 *COI* sequences, including 14 from GenBank, with a length of 703 bp were aligned. Additionally, 46 specimens with *28S* combined data, ranging from 630 to 631 bp in length, were included in the analysis. The *COI* phylogenetic tree revealed the presence of five clades, with each being supported by high values of both ML ultrafast bootstrap and BI posterior probability (Fig. 1). Contrastingly, the *28S* phylogenetic tree showed only four clades, with wasps reared from figs of *F. subpisocarpa* and *F. caulocarpa* being combined into one clade (Fig. S1). Most clades in the *COI* tree exhibited a strong association with specific fig species, except for two cases involving *F. microcarpa* and *F.*

benjamina, which shared *Sycoscapter* wasp species. This observation was also reflected in the *COI+28S* combined data, where five clades corresponding to *Sycoscapter* wasps associated with Taiwanese monoecious figs could be discerned (Fig. 2).

Despite the distinct and well-supported separation of the *Sycoscapter* species in Taiwanese monoecious figs, incongruence in tree topology was observed between the tree constructed using the *COI* gene and that constructed using *COI+28S* data. For example, in the *COI* tree, Clade II appeared as a sister lineage to the group consisting of Clade III-V, then diverged from Clade I. In contrast, the tree based on *COI+28S* combined data grouped Clade II with Clade III. This incongruence was further supported by the relatively low values of both ML ultrafast bootstrap and BI posterior probability (Figs. 1 and 2).

In addition to the genetic distances of 6.69–9.95%

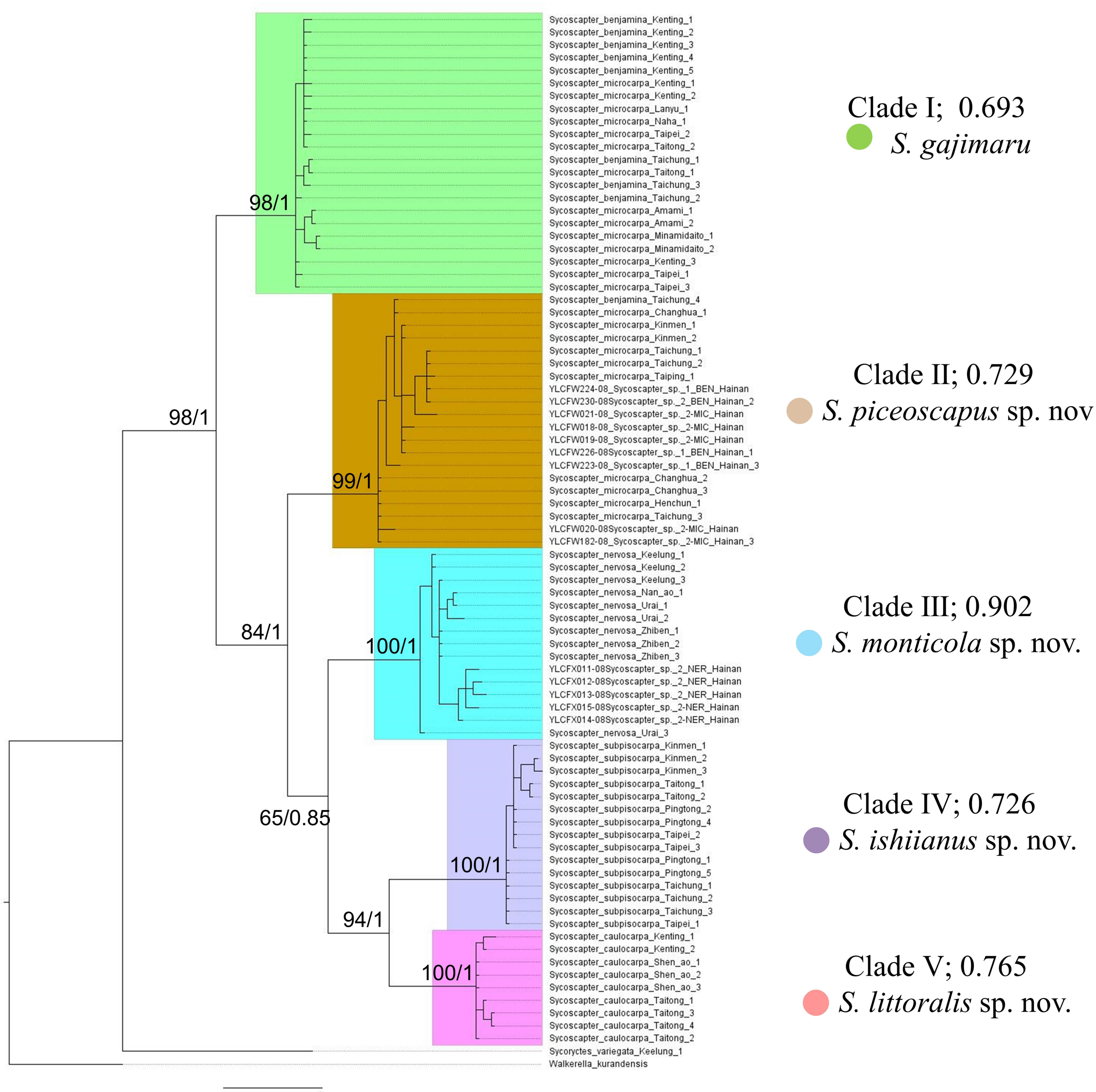

Fig. 1. Phylogenetic tree of the *Sycoscapter* species associated with monoecious figs in Taiwan and other congeners based on *COI* genes. The values at the nodes are the ultrafast bootstraps and posterior possibilities for maximum likelihood (ML) and Bayesian inference (BI) analyses, respectively. The number of each clade indicates the support value of the bPTP model.

among species and 0.57–0.72% within species (Table 1), support values of the bPTP model (0.693–0.902) further supported the notion that the *Sycoscapter* wasps in this study represent five distinct species (Fig.1). Therefore, based on genetic differentiation and the topology of the phylogenetic tree reconstructed using *COI+28S* combined data, it is evident that five *Sycoscapter* species, corresponding to five clades, associated with monoecious figs exist in Taiwan, namely *Sycoscapter gajimaru* (Ishii), *Sycoscapter piceoscapus* Chou et Tzeng sp. nov., *Sycoscapter monticola* Chou et Tzeng sp. nov., *Sycoscapter ishiianus* Chou et Tzeng sp. nov.,

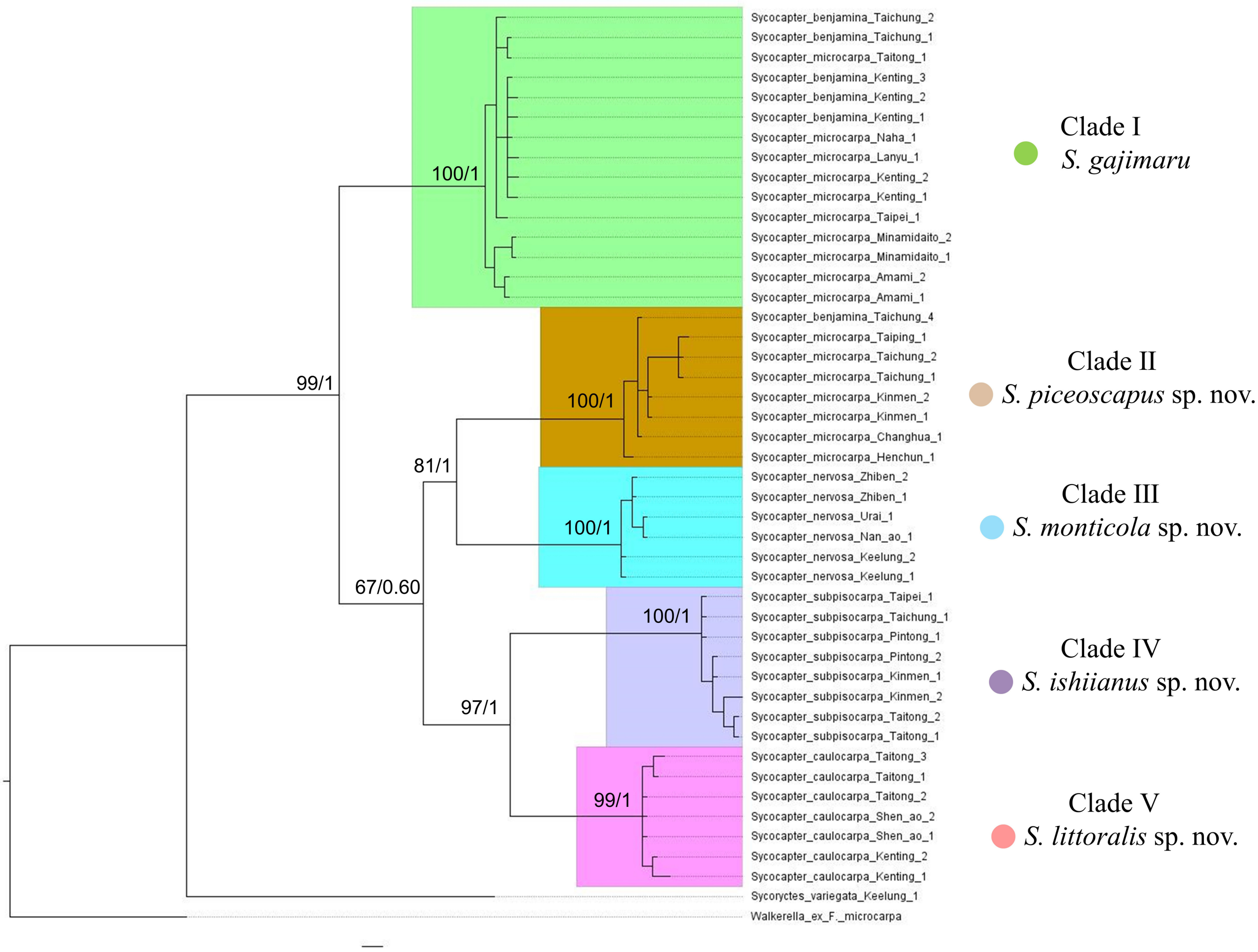

Fig. 2. Phylogenetic tree of the *Sycoscapter* species associated with monoecious figs in Taiwan based on *COI+28S* combined data. The values at the nodes are the ultrafast bootstraps and posterior possibilities for maximum likelihood (ML) and Bayesian inference (BI) analyses, respectively.

Table 1. Percentage of pairwise nucleotide divergences with Kimura 2-parameter (K2P) distances and number of base pair differences based on the *COI* gene within and between species of *Sycoscapter* wasps associated with monoecious figs in Taiwan. In the inter-species column, the lower-left values are K2P distances and upper-right are bp differences

	Intra-species		Inter-species				
	Nucleotide divergence	Base pair difference	*S. gajimaru*	*S. piceoscapus*	*S. monticola*	*S. ishiianus*	*S. littoralis*
S. gajimaru	4	0.57		49	47	63	53
S. piceoscapus	5	0.72	7.32		48	52	50
S. monticola	4	0.57	7.01	7.16		53	45
S. ishiianus	4	0.57	9.55	7.79	7.95		43
S. littoralis	4	0.57	7.96	7.48	6.69	6.39	

and *Sycoscapter littoralis* Chou et Tzeng sp. nov.

In terms of morphological observation, each species could be readily identified as a member of *Sycoscapter* by specific characteristics, such as symmetric funicles and a "boot-like" stigma on the forewing in females, and two terga in dorsal view and a non-enlarged basitarsus on the hind legs in males. Comparative analyses with other related *Sycoscapter* species revealed that Taiwanese species could be categorized into four morpho-groups based on similarities in male head-shape morphology. *Sycoscapter gajimaru*, for instance, clustered with *Sycoscapter stabilis* (Walker) and *Sycoscapter benghalensis* Pramanik and Dey owing to similarities in male head shape (rectangular with curved lateral margins). However, these species still differed based on other characters, such as vertex shape, setae number on female forewings, and malar L/eye L ratio in males (Table 2). As shown in table 3, *S. piceoscapus* and *S. benghalensis* Pramanik and Dey formed a morpho-group owing to shared characteristics, such as ovate head shape and large compound eyes in males, although they could be differentiated based on female characters, including vertex shape and scape coloration. *Sycoscapter monticola* exhibited a unique subhexagonal head shape in males, setting it apart from *Sycoscapter vijayaii* Priyadarsanan, although both share the same host fig species. Moreover, there were distinguishing features in male antennal segments (Table 4). The last group encompassed three species, namely *S. ishiianus*, *S. infectorius* (Joseph), and *S. littoralis*, which exhibited a long rectangular head shape with straight lateral margins. However, they could be distinguished through various characters, including head shape, maxillary palp segment in females, and the spur on the fore tibia in males (Table 5).

Table 2. Comparison of morphological characters between *Sycoscapter gajimru* (Ishii), *S. stabilis* (Walker) and *S. benghalensis* Pramanik and Dey

	S. gajimaru	*S. stabilis*	*S. benghalensis*
Female			
POL/ OOL	8.05	≥ 9	9
Vertex	concave	straight	straight
Head H/ head W	0.79	0.83	1.3
Seta on forewing	5–7 in 2 rows	10 in 1 row	23 in 4 rows
Marginal vein L/ stigmal vein L	3	1.7	1.7
Ovipositor L/ metasoma L	4.03	5.3	4.7
Male			
Head L/ head W	1.18	0.85-1.21	1
Malar L/ eye L	1.79	1.52	1
Mandible L/ mandible W	2.3	1.7	2.7

Characters of *S. stabilis* referred to Pramanik and Dey (2019) and Wiebes (1967) and that of *S. benghalensis* referred to Pramanik and Dey (2019).

Table 3. Comparison of morphological characters between *Sycoscapter picescapus* sp. nov. and *S. benjaminae* Pramanik and Dey

	S. piceoscapus	*S. benjaminae*
Female		
POL/ OOL	7.07	6
Vertex	concave	straight
Scape coloration	black	yellow
Sculpture on antennal scrobes	reticulate	psilate
Seta on forewing	7–10 in 2 rows	11 in 4 rows
Marginal vein L/ stigmal vein L	2.3	1.7
Ovipositor L/ metasoma L	4.75	4.6
Male		
Wing vestigial L/ mesosoma L	1.39	1.7

Characters of *S. benjaminae* referred to Pramanik and Dey (2019).

In addition to head shape in males, the presence or absence of rudimentary wing vestiges in males could also be used to categorize *Sycoscapter* wasps into two morpho-groups. Notably, wasps possessing rudimentary wing vestiges were exclusively associated with monoecious figs, whereas those lacking vestiges were associated with functional dioecious figs.

TAXONOMY

Family Pteromalidae Dalman, 1820
Genus *Sycoscapter* Saunders, 1883

Sycoscapter gajimaru (Ishii, 1934)
(Figs. 3, 4, 5)

Goniogaster gajimaru Ishii, 1934: 89, pls. 2(20).
Sycoscapter gajimaru Wiebes, 1964: 83 (Japan); Yokoyama and Iwatsuki, 1998: 43 (Japan); Chen et al. 1999: 73, fig. 19 (Taiwan); Karube et al. 2022: 51, fig. 43 (Kita-Iwo, Japan; introduced).

Type locality: Naha, Okinawa, Japan.

Material examined: **Lectotype**: 1♀, Naha, Okinawa, 22-III-1934, Col. T. Ishii (NARO), designated here. Others: **Japan**: 1♀1♂, Naha (26.226520, 127.713802), Okinawa, ex *Ficus microcarpa* L. f., 3-VI-2023, leg. P. A. Chou (NCHU); 1♀, Amami (28.391214, 129.506937), Kagoshima, ex *Ficus microcarpa* L. f., 9-V-2021, leg. K. Arimoto (NCHU); 1♀, Minamidaito (25.836189, 131.237121), Okinawa, ex *Ficus microcarpa* L. f., 20-V-2022, leg. K. Arimoto (NCHU). **Taiwan**: 1♂1♀, Fugui Cape (25.292583, 121.538262), New Taipei City, ex *Ficus microcarpa* L. f., 13-IX-2020, leg. P. A. Chou (NCHU); 1♀, National Taiwan University, Taipei City, ex *Ficus microcarpa* L. f., 6-IX-1991, leg. C. F. Hsu (TARI); 1♀, Taichung Park, Taichung City, ex *Ficus microcarpa* L. f., 15-IX-1991, leg. K. S. Lin (TARI); 1♀, Wanfeng, Taichung City, ex *Ficus microcarpa* L. f., 8-X-1991, leg. K. S. Lin (TARI); 1♂1♀, Botanical Garden of National Museum of Natural Science (24.158742, 120.667746), Taichung

Table 4. Comparison of morphological characters between *Sycoscapter monticola* sp. nov. and *S. vijayaii* Priyadarsanan

	S. monticola	*S. vijayaii*
Female		
POL/ OOL	4.84	11
Seta on forewing	4–11 in 2 rows	7–10 in 1 row
Marginal vein L/ stigmal vein L	2	1.5
Ovipositor L/ metasoma L	6.08	7
Male		
Head shape	subhexagonal	rectangular
Claval segment	3	2

Characters of *S. vijayaii* referred to Priyadarsanan (2000) and Pramanik and Dey (2019).

Table 5. Comparison of morphological characters between *Sycoscapter ishiianus* sp. nov., *S. infectorius* (Joseph) and *S. littoralis* sp. nov.

	S. ishiianus	*S. infectorius*	*S. littoralis*
Female			
POL/ OOL	5.59	6.7	5.35
Maxillary palp	4	3	4
Head shape	obcordate	obcordate	rounded
Seta on forewing	9–13 in 3 rows	15 in 3 rows	9–10 in 3 rows
Marginal vein L/ stigmal vein L	2.6	unknown	2.6
Ovipositor L/ metasoma L	4.37	5.6	3.76
Male			
Pronotum shape	subpentagonal	unknown	oblong
Fore spur exceeds last tarsomere	no	yes	no

Characters of *S. infectorius* referred to Joseph (1953 1961) and Pramanik and Dey (2019).

City, ex *Ficus benjamina* L. var. *bracteata* Corner, 27-IV-2023, leg. P. A. Chou (NCHU); 1♀, Yuanlin Park, Changhua, ex *Ficus microcarpa* L. f., 13-IX-1991, leg. K. S. Lin (TARI); 1♀, Tsaotun, Nantou, ex *Ficus microcarpa* L. f., 8-X-1991, leg. K. S. Lin (TARI); 1♀, Kenting Forest Recreation Area (21.961888, 120.814306), Pingtung, ex *Ficus microcarpa* L. f., 11-VIII-2022, leg. P. A. Chou (NCHU); 1♂1♀, Kenting Forest Recreation Area (21.964254, 120810716), Pingtung, ex *Ficus benjamina* L. var. *bracteata* Corner, 11-VIII-2022, leg. P. A. Chou (NCHU); 1♀, Tali, Ilan, ex *Ficus microcarpa* L. f., 14-IX-1991, leg. T. F. Hsu (TARI); 1♂1♀, Shitiping (23.491086, 121.508953), Hualien, ex *Ficus microcarpa* L. f., 29-VIII-2018, leg. P. A. Chou (NCHU); 1♂1♀, Taitung Seashore Park (22.751414, 121.610591), Taitung, ex *Ficus microcarpa* L. f., 25-III-2023, leg. P. A. Chou (NCHU); 1♂1♀, Ludao (22.671815, 121.505912), Taitung, ex *Ficus microcarpa* L. f., 30-VIII-2018, leg. P. A. Chou (NCHU).

Description: Female: Whole L = 3.82–4.93 mm with body L = 1.08–1.43 mm and ovipositor sheath L = 2.74–3.50 mm. Body metallic green (Fig. 3C). Compound eyes pale red (Fig. 3A). Antenna scape and pedicel yellow, anelli, funicle and clava black (Fig. 3I). Legs yellow (Fig. 3J, 3L, 3N) except for the basal part of hind coxa black in antiaxial view (Fig. 3N).

Head: Obcordate in front view (Fig. 3A); H = 0.26 mm, W over compound eyes = 0.32 mm, W between compound eyes = 0.22 mm. Compound eye H 1.5× malar space L, and 3× compound eyes W. POL 7.49× OOL. Clypeus margin with a thin projection in the middle (Fig. 4A). Face and antennal scrobes with raised reticulation (Fig. 3A). Mandible bidentate (Fig. 3G). Maxillary palp 3-segmented; length ratio = 3:4:4 (Fig. 4B). Labial palp 2-segmented; length ratio = 3:2 (Fig. 4B). The distance between toruli 0.3× clypeus margin. Antennal formula 11253 and L = 0.49 mm; length ratio of scape, pedicel, anelli, funicle and clava = 14:4:1:20:10 (Fig. 3I). Scape L 3.85× W, with sparse trichoid sensillae (Fig. 4C). Pedicel L 1.3× W, with sparse trichoid sensillae (Fig. 4C). Both anelli equal in length and the second one wider (Fig. 4C). All funicular segments equal in length; the first funicular segment L 0.92× W, with 3 multiporous placoid sensillae and 8 chaetica sensillae in antiaxial view; the chaetica sensilla longer than funicular segment (Fig. 4C). Claval segments slightly wider than funicular segments; the first claval segment L 0.76× W, with 3 multiporous placoid sensillae and 7 chaetica sensillae in antiaxial view.

Mesosoma: Mesosoma L = 0.41 mm, W = 0.29 mm; length ratio of pronotum, scutum, scutellum and propodeum = 2:4:5:1. Pronotum, scutum and scutellum with raised reticulation but propodeum psilate (Fig. 3B) Pronotum with collar in ventral view. Scutum with incomplete notauli (Fig. 3B). Scutellum nearly as wide as long; punctures of reticulation rounded (Fig. 4D). Metanotum strongly compressed and the middle covered by scutellum. Propodeum transverse with two longitudinal keels. Forewing L = 1.01 mm, W = 0.44 mm, with 5–7 setae below the marginal vein; length ratio of submarginal vein, marginal vein, postmarginal vein and stigmal vein = 5:3:4:2 (Fig. 3P). Hind wing L = 0.58 mm, W = 0.12 mm; length ratio of submarginal vein and marginal vein = 2:3. Foreleg L = 0.65 mm; length ratio of coxa, trochanter, femur, tibia and tarsus = 3:2:5:4:3 (Fig. 3J). Fore tibia with a curve, bidentate spur reaching the apex of first tarsomere; 1 spine beside spur in both axial and antiaxial views (Fig. 4E, 4F). Fore tarsus 5-segmented; length ratio of each segment = 4:3:3:2:7. Mid leg L = 0.67 mm; length ratio of coxa, trochanter, femur, tibia and tarsus = 1:1:3:4:3 (Fig. 3L). Mid tibia with a straight spur; spur L 0.5× the first tarsomere L; 1 spine beside spur in axial view but no spine in antiaxial view (Fig. 4G, 4H). Mid tarsus 5-segmented; length ratio of each segment = 7:4:3:2:4. Hind leg L = 0.92 mm; length ratio of coxa, trochanter, femur, tibia and tarsus = 3:1:4:5:3 (Fig. 3N). Hind tibia with a straight spur; spur L 0.5× the first tarsomere L; 19-24 teeth in axial view and 3 spines beside spur in antiaxial view (Fig. 4I, 4J). Hind tarsus 5-segmented; length ratio of each segment = 8:4:3:2:5.

Metasoma: Abdomen without ovipositor sheath L = 0.74 mm.

Male: L = 1.33–1.40 mm. Body brown (Fig. 3D). Eyes black (Fig. 3E). Mandible dark brown (Fig. 3H). Antenna pale yellow (Fig. 3E). Legs brown (Fig. 3K, 3M, 3O).

Head: Rectangular shape in dorsal view (Fig. 3E); L without mandible = 0.45 mm, W = 0.38 mm. Mandible L = 0.25 mm, W = 0.10 mm. Mandible falcate with a fine tooth in the middle (Fig 3H). Clypeus margin concave in the middle. Maxillary palp 4-segmented; length ratio = 3:3:1:3 (Fig. 5B). Labial palp 2-segmented; length ratio = 3:2 (Fig. 5B). Compound eye L 2.5× W. Malar space L 1.79× compound eye L. Toruli close to clypeus margin. Antennal formula 11153 and L = 0.37 mm; length ratio of scape, pedicel, anellus, funicle and clava = 11:7:1:8:7. Scape L 2.51× W, with sparse trichoid sensillae (Fig. 5A). Pedicel L 3.32× W, with sparse trichoid sensillae (Fig. 5A). The first and third funicular segment swollen, L 0.6× W; other funicular segments L 0.55× W; all funicular segments with trichoid sensillae (Fig. 5A). Claval segments as wide as the swollen funicular segments; the first claval segment L 0.9× W, with trichoid sensillae and multiporus placoid sensillae (Fig. 5A).

Mesosoma: Long pentagon in dorsal view (Fig.

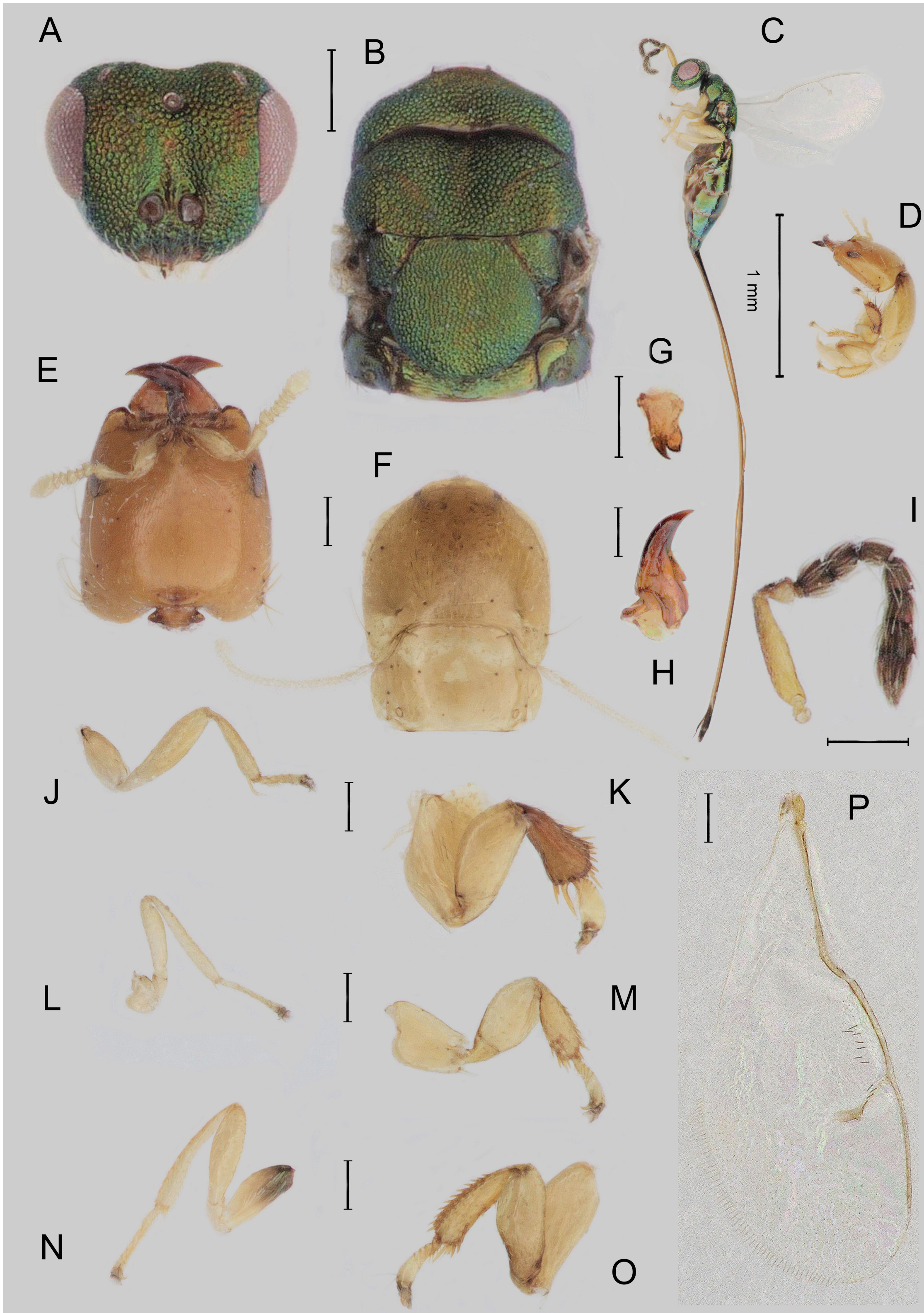

Fig. 3. *Sycoscapter gajimaru* (Ishii, 1934). A, Female head, front; B, Female mesosoma, dorsal; C, Female habitus, lateral; D, Male habitus, lateral; E, Male head, dorsal; F, Male mesosoma, dorsal; G, Female left mandible, ventral; H, Male left mandible, dorsal; I, Female antenna; J, Female right foreleg; K, Male right foreleg; L, Female right mid leg; M, Male right mid leg; N, Female right hind leg; O, Male right hind leg; P, Female forewing. Scale bar = 0.1 mm if no number is noted.

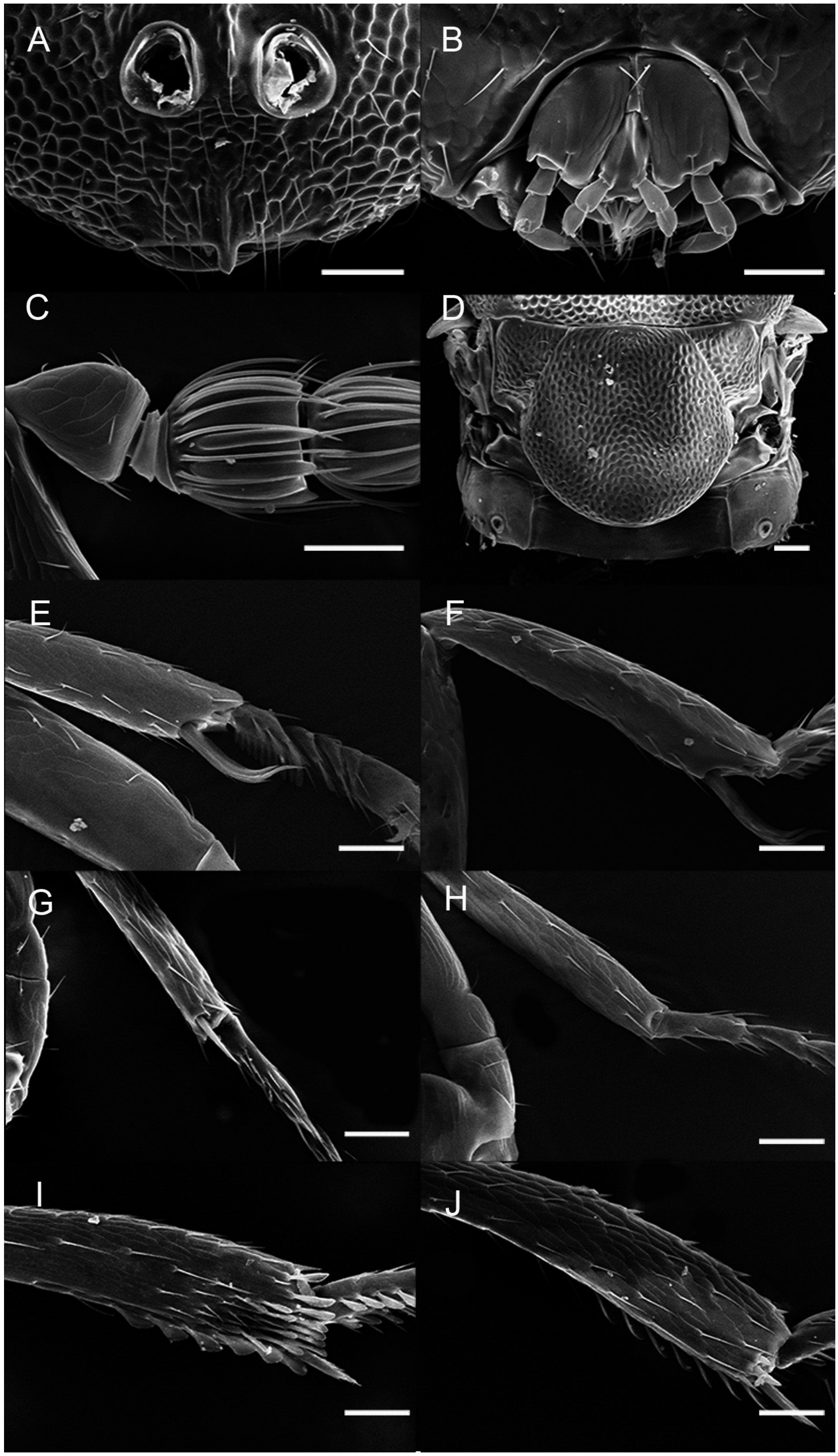

Fig. 4. Scanning electron images of female *Sycoscapter gajimaru* (Ishii, 1934). A, Toruli and epistomal margin; B, Maxillary palps and labial palps; C, Anelli and the first funiculus; D, Scutellum; E, Left fore tibia, axial; F, Right tibia, antiaxial; G, Left mid tibia, axial; H, Right mid tibia, antiaxial; I, Right hind tibia, axial; J, Left hind tibia, antiaxial. Scale bar = 0.03 mm.

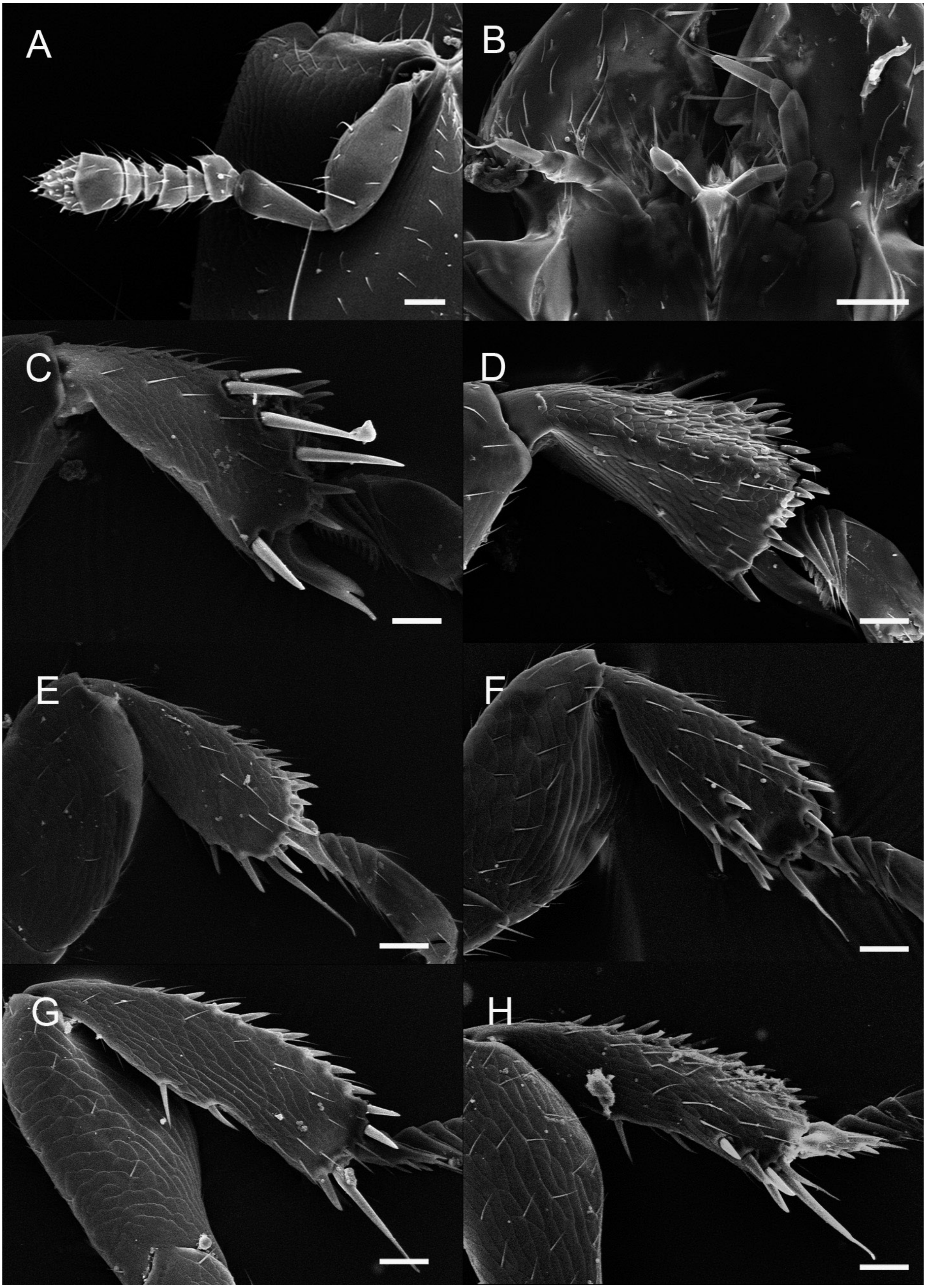

Fig. 5. Scanning electron images of male *Sycoscapter gakimaru* (Ishii, 1934). A, Antenna; B, Maxillary palps and labial palps; C, Left fore tibia, axial; D, Right tibia, antiaxial; E, Left mid tibia, axial; F, Right mid tibia, antiaxial; G, Right hind tibia, axial; H, Left hind tibia, antiaxial. Scale bar = 0.03 mm.

3F); L = 0.54 mm, W = 0.39 mm; length ratio of pronotum and the fused tergum = 4:3. Pronotum with collar in ventral view. Mesonotum, metanotum and propodeum fused in dorsal view (Fig. 3F). Rudimentary wing vestige present, L = 0.39 mm (Fig. 3F). Foreleg L = 0.85 mm; length ratio of coxa, trochanter, femur, tibia and tarsus = 4:1:3:3:2 (Fig. 3K). Fore tibia with a slightly curve, bidentate spur reaching the last tarsomere; 11–12 spines in axial view and 15–16 spines in antiaxial view (Fig. 5C, 5D). Fore tarsus 5-segmented; length ratio of each segment = 2:1:1:1:10. Mid leg L = 0.67 mm; length ratio of coxa, trochanter, femur, tibia and tarsus = 2:1:2:2:2 (Fig. 3M). Mid tibia with a straight spur reaching the fourth tarsomere; 13 spines in axial view and 12–13 spines in antiaxial view (Fig. 5E, 5F). Mid tarsus 5-segmented; length ratio of each segment = 2:1:1:1:6. Hind leg L = 0.92 mm; length ratio of coxa, trochanter, femur, tibia and tarsus = 7:2:5:6:4 (Fig. 3O). Hind tibia with a straight spur reaching the fourth tarsomere; 15–18 spines in axial view and 23 spines in antiaxial view (Fig. 5G, 5H). Hind tarsus 5-segmented; length ratio of each segment = 1:1:1:1:4.

Metasoma: Abdomen L = 0.53 mm.

Host: *Ficus microcarpa* L. f. and *Ficus benjamina* L. var. *bracteata* Corner.

Distubution: Taiwan; Japan: Ryukyu islands and Kita-Iwo (introduced).

Diagnosis: This species is similar to *S. benghalansis* Pramanik and Dey but can be distinguished by the characters, following the key provided by Pramanik and Dey (2019), in female including the seta number on forewing (5–7 in *S. gajimaru* vs. 23 in *S. benghalensis*), the ratio of ovipositor L to metasoma L (4.03 in *S. gajimaru* vs. 4.7 in *S. benghalensis*); in male including the ratio of malar space L to eye L (1.79 in *S. gajimaru* vs. 1 in *S. benghalensis*). This species is also similar to *S. stabilis* (Walker) but can be distinguished by the characters in female including the ratio of ovipositor to metasoma (4.03 in *S. gajimaru* vs. 5.3 in *S. stabilis*) and vertex shape (concave in *S. gajimaru* vs. straight in *S. stabilis*); in male including the ratio of mandible L to W (2.3 in *S. gajimaru* vs. 1.7 in *S. stabilis*). Despite the differences above, ambiguous delimitation between males of *S. gajimaru* and *S. stabilis* still exists, with males of the latter species reported to have variable characters (Wiebes 1967).

Remarks: Ishii (1934) published two *Sycoscapter* species, *S. inubiae* (= *Goniogaster inubiae*) and *S. gajimaru* (= *G. gajimaru*). In that description, the projection on clypeus margin of the former was sharp while that of the latter was thin. However, the figures showed the projection of *S. inubiae* [Ishii (1934): Fig. 12] was thinner than that of *S. gajimau* [Ishii (1934): Fig. 20]. After examining samples of *S. gajimaru* and *S. inubiae*, we think figures of the two species were numbered mistakenly.

Ishii (1934) did not designate the holotype of *Sycoscapter gajimaru* (= *Goniogaster gajimaru*), but only one specimen with the same collection information was found in NARO. Therefore, this specimen should be designated as the lectotype. Since this species could be distinguished from others by the characters of the mesosoma, this lectotype could present its diagnostic characters even if in the headless condition (Fig. S2).

Sycoscapter piceoscapus **Chou & Tzeng sp. nov.**

(Figs. 6, 7, 8)
urn:lsid:zoobank.org:act:BF014E39-A51E-43EC-B264-B4AB83AFCAB5

Type locality: National Chung-Hsing University, Taichung, Taiwan.

Material examined: Holotype: 1♀, National Chung-Hsing University (24.122583, 120.677985), Taichung, ex *Ficus microcarpa* L. f., 17-II-2020, leg. P. A. Chou (NCHU). Paratypes: 1♂, National Chung-Hsing University (24.122583, 120.677985), Taichung, ex *Ficus microcarpa* L. f., 17-II-2020, leg. P. A. Chou (NCHU); 1♂1♀, Botanical Garden of National Museum of Natural Science (24.158790, 120.667772), Taichung City, ex *Ficus microcarpa* L. f., 7-VII-2018, leg. P. A. Chou (TARI). Others: **Taiwan**: 1♀, National Chiao Tung University (24.789220, 121.000047), Hsinchu, ex *Ficus microcarpa* L. f., 20-X-2022, leg. C. Y. Huang (NCHU); 1♂1♀, National Chung-Hsing University (24.122583, 120.677985), Taichung, ex *Ficus microcarpa* L. f., 8-III-2019, leg. P. A. Chou (NCHU); 1♂1♀, Taipin (24.116256, 120.732507), Taichung City, ex *Ficus microcarpa* L. f., 7-IV-2023, leg. C. Y. Huang (NCHU); 1♂1♀, Changhua City (24.083587, 120.556162), Chunghua, ex *Ficus microcarpa* L. f., 9-VIII-2022, leg. C. Y. Huang (NCHU); 1♂1♀, Botanical Garden of National Museum of Natural Science (24.158742, 120.667746), Taichung City, ex *Ficus benjamina* L. var. *bracteata* Corner, 27-IV-2023, leg. P. A. Chou (NCHU); 1♂1♀, Mt. Wuhu (24.501129, 118.437810), Kinmen, ex *Ficus microcarpa* L. f., 4-VIII-2021, leg. P. A. Chou (NCHU). **China**: 1♂1♀, South China National Botanical Garden (23.183609, 113.370332), Guangdong Prov. ex *Ficus microcarpa* L. f., 16-XII-2018, leg. P. A. Chou (NCHU). 8♂4♀, Danzhou (19.52, 109.57), Hainan Prov. ex *Ficus microcarpa* L. f., 24-IV-2004, col. G. Feng, W. Li, H. Y. Hu, L. M. Niu (CAS) (examined from online photographs); 10♂10♀, Zhuang (19.747, 109.411), Hainan Prov., ex *Ficus benjamina* L., 24-IV-2004, col. G. Feng, W. Li, H. Y. Hu, L. M. Niu (CAS) (examined from online photographs).

Description: Female: Whole L = 3.65–4.08 mm with body L = 0.95–1.08 mm and ovipositor sheath L = 2.69–3.0 mm. Body metallic green (Fig. 6C). Compound eyes pale red (Fig. 6A). Antenna black with yellow coloration on the basal part of the scape (Fig. 6I). Legs yellow (Fig. 6J, 6L, 6N); middle of mid femur slightly black in antiaxial view (Fig. 6L); basal part of hind coxa black in antiaxial view (Fig. 6N).

Head: Obcordate in front view (Fig. 6A); H = 0.25 mm, W over compound eyes = 0.34 mm, W between compound eyes = 0.23 mm. Compound eye H = 1.28× malar space, and 2.59× compound eye W. POL 7.07× OOL. Clypeus margin with a thin and blunt projection in the middle (Fig. 7A). Face and antennal scrobes with raised reticulation (Fig. 6A). Mandible bidentate (Fig. 6G). Maxillary palp 3-segmented, length ratio = 2:3:5 (Fig. 7B). Labial palp 2-segmented, length ratio = 3:2 (Fig. 7B). The distance between toruli 0.33× clypeus margin. Antennal formula 11253 and L = 0.51 mm; length ratio of scape, pedicel, anelli, funicle and clava = 14:4:1:20:10 (Fig. 6I). Scape L 5.34× W, with sparse trichoid sensillae (Fig. 7C). Pedicel L 1.18× W, with sparse trichoid sensillae (Fig. 7C). Both anelli equal in length and the second one wider (Fig. 7C). All funicular segments equal in length; the first funicular segment L 0.81× W, with 2 multiporous placoid sensillae and 6 chaetica sensillae in antiaxial view; the chaetica sensilla longer than funicular segment (Fig. 7C). Claval segments slightly wider than funicular segments. The first claval segments L 0.81× W, with 3 multiporous placoid sensillae and 6 chaetica sensillae in antiaxial view.

Mesosoma: Mesosoma L = 0.36 mm, W = 0.26 mm; length ratio of pronotum, scutum, scutellum and propodeum = 2:5:8:2. Pronotum, scutum and scutellum with raised reticulation but propodeum psilate in dorsal view (Fig. 6B) Pronotum with collar in ventral view. Scutum with incomplete notauli (Fig. 6B). Scutellum nearly as wide as long, punctures of reticulation lengthened longitudinally (Fig. 7D). Metanotum strongly compressed and the middle covered by scutellum. Propodeum transverse, with two longitudinal keels. Forewing L = 1.09 mm, W = 0.46 mm, with 7–10 setae below the marginal vein; length ratio of submarginal vein, marginal vein, postmarginal vein and stigmal vein = 5:3:4:2 (Fig. 6P). Hind wing L = 0.75 mm, W = 0.18 mm; length ratio of submarginal vein and marginal vein =2:3. Foreleg L = 0.61 mm; length ratio of coxa, trochanter, femur, tibia and tarsus = 3:2:5:4:3 (Fig. 6J). Fore tibia with a curve, bidentate spur reaching the apex of first tarsomere; 2 spines beside spur in axial view and 2 spines in antiaxial view (Fig. 7E, 7F). Fore tarsus 5-segmented; length ratio of each segment = 4:3:3:2:7. Mid leg L = 0.63 mm; length ratio of coxa, trochanter, femur, tibia and tarsus = 1:1:3:4:3 (Fig. 6L). Mid tibia with a straight spur; spur L 0.5× the first tarsomere L; 1 spine beside spur in axial view but no spine in antiaxial view (Fig. 7G, 7H). Mid tarsus 5-segmented; length ratio of each segment = 7:4:3:2:4. Hind leg L = 0.84 mm; length ratio of coxa, trochanter, femur, tibia and tarsus = 3:1:4:5:3 (Fig. 6N). Hind tibia with a straight spur; spur L 0.5× the first tarsomere L; 21-23 teeth in axial view and 2 spines beside spur in antiaxial view (Fig. 7I, 7J). Hind tarsus 5-segmented; length ratio of each segment = 8:4:3:2:5.

Metasoma: Abdomen without ovipositor sheath L = 0.57 mm.

Male: L = 1.22–1.30 mm. Body brown (Fig. 6D). Eyes black (Fig. 6E). Mandible dark brown (Fig. 6H). Antenna pale yellow (Fig. 6E). Legs brown (Fig. 6K, 6M, 6O).

Head: Long ovate in dorsal view (Fig. 6E); L without mandible = 0.40 mm, W = 0.35 mm. Mandible L = 0.22 mm, W = 0.1 mm. Mandible falcate with a fine tooth at the middle (Fig 6H). Clypeus margin concave in the middle. Maxillary palp 4-segmented, length ratio = 3:3:1:2 (Fig. 8B). Labial palp 2-segmented, length ratio = 3:2 (Fig. 8B). Compound Eye L 3.5× W. Malar space L 1.03× compound eye L. Toruli close to clypeus margin. Antennal formula 11153 and L = 0.34 mm; length ratio of scape, pedicel, anellus, funicle and clava = 13:7:1:8:7. Scape L 3.35× W, with sparse trichoid sensillae (Fig. 8A). Pedicel L 2.78× W, with sparse trichoid sensillae (Fig. 8A). The first and third funicular segments swollen, L 0.55× W; other funicular segments L 0.47× W. All funicular segments with trichoid sensillae (Fig. 8A). Claval segments as wide as the swollen funicular segments, the first segment L 0.88× W, with trichoid sensillae and multiporus placoid sensillae (Fig. 8A).

Mesosoma: Oblong in dorsal view (Fig. 6F). L = 0.46 mm, W = 0.34 mm; length ratio of pronotum and the fused tergum = 3:2. Pronotum with collar in ventral view. Mesonotum, metanotum and propodeum fused in dorsal view (Fig. 6F). Rudimentary wing vestige present, L = 0.33 mm (Fig. 6F). Foreleg L = 0.81 mm; length ratio of coxa, trochanter, femur, tibia and tarsus = 4:1:3:3:2 (Fig. 6K). Fore tibia with a slightly curve, bidentate spur reaching the last tarsomere; 5–6 spines in axial view and 10–14 spines in antiaxial view (Fig. 8C, 8D). Fore tarsus 5-segmented; length ratio of each segment = 2:1:1:1:6. Mid leg L = 0.69 mm; length ratio of coxa, trochanter, femur, tibia and tarsus L = 2:1:2:2:2 (Fig. 6M). Mid tibia with a straight spur reaching the second tarsomere; 8 spines in axial view and 13–14 spines in antiaxial view (Fig. 8E, 8F). Mid tarsus 5-segmented; length ratio of each segment = 1:1:1:1:5.

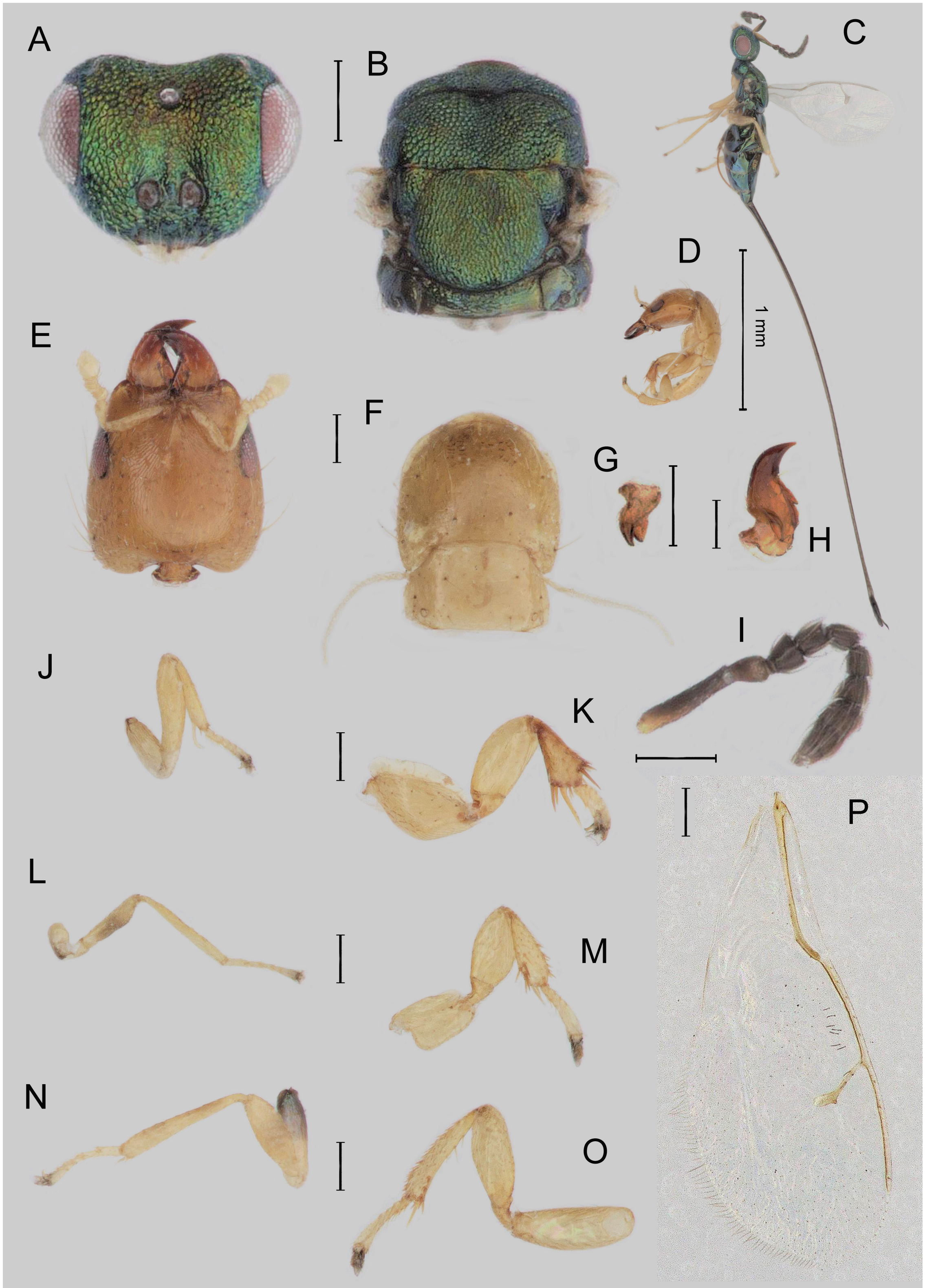

Fig. 6. *Sycoscapter piceoscapus* sp. nov. A, Female head, front; B, Female mesosoma, dorsal; C, Female habitus, lateral; D, Male habitus, lateral; E, Male head, dorsal; F, Male mesosoma, dorsal; G, Female left mandible, ventral; H, Male left mandible, dorsal; I, Female antenna; J, Female right foreleg; K, Male right foreleg; L, Female right mid leg; M, Male right mid leg; N, Female right hind leg; O, Male right hind leg; P, Female forewing. Scale bar = 0.1 mm if no number is noted.

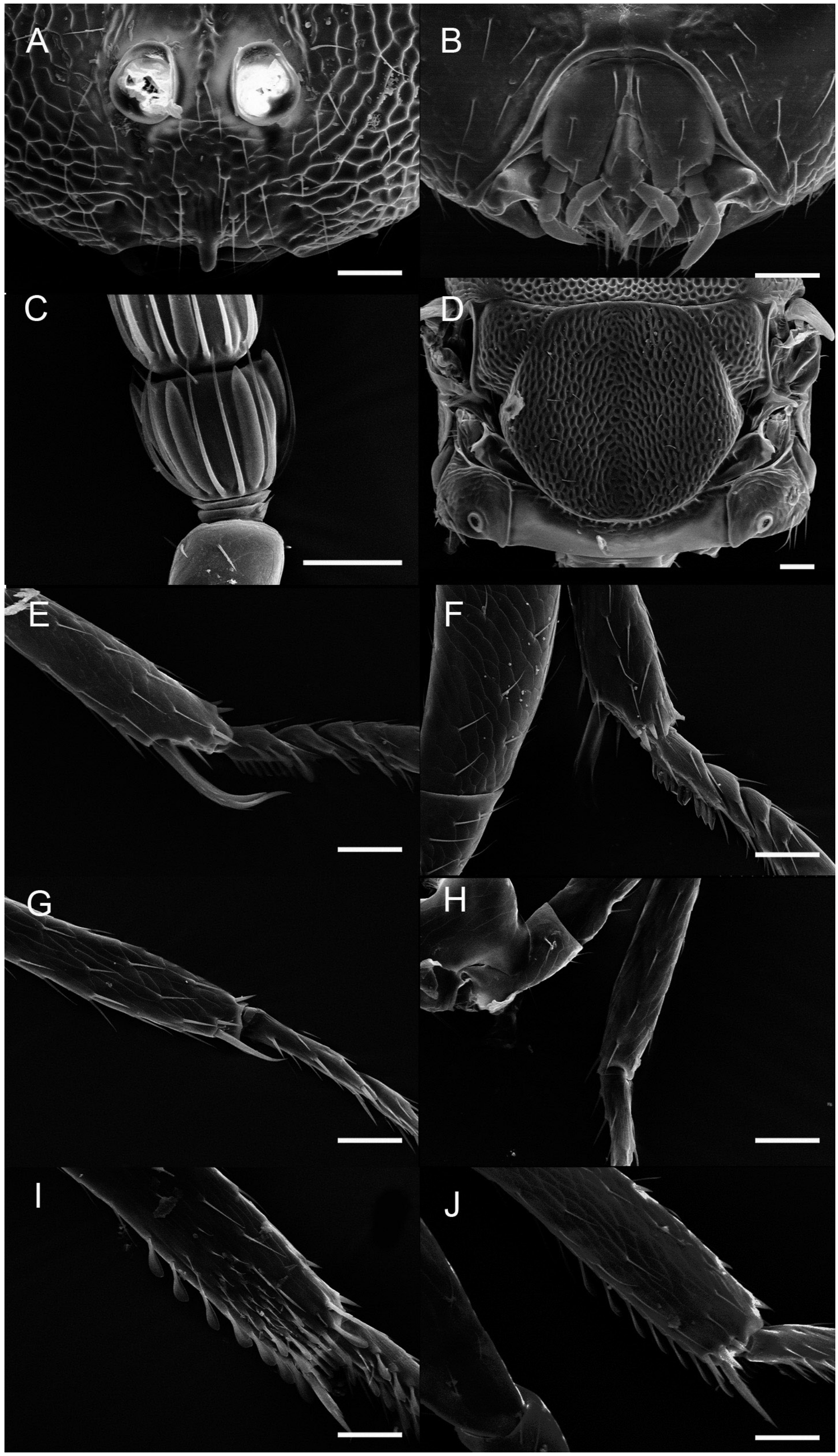

Fig. 7. Scanning electron images of female *Sycoscapter piceoscapus* sp. nov. A, Toruli and epistomal margin; B, Maxillary palps and labial palps; C, Anelli and the first funiculus; D, Scutellum; E, Left fore tibia, axial; F, Right tibia, antiaxial; G, Left mid tibia, axial; H, Right mid tibia, antiaxial; I, Right hind tibia, axial; J, Left hind tibia, antiaxial. Scale bar = 0.03 mm.

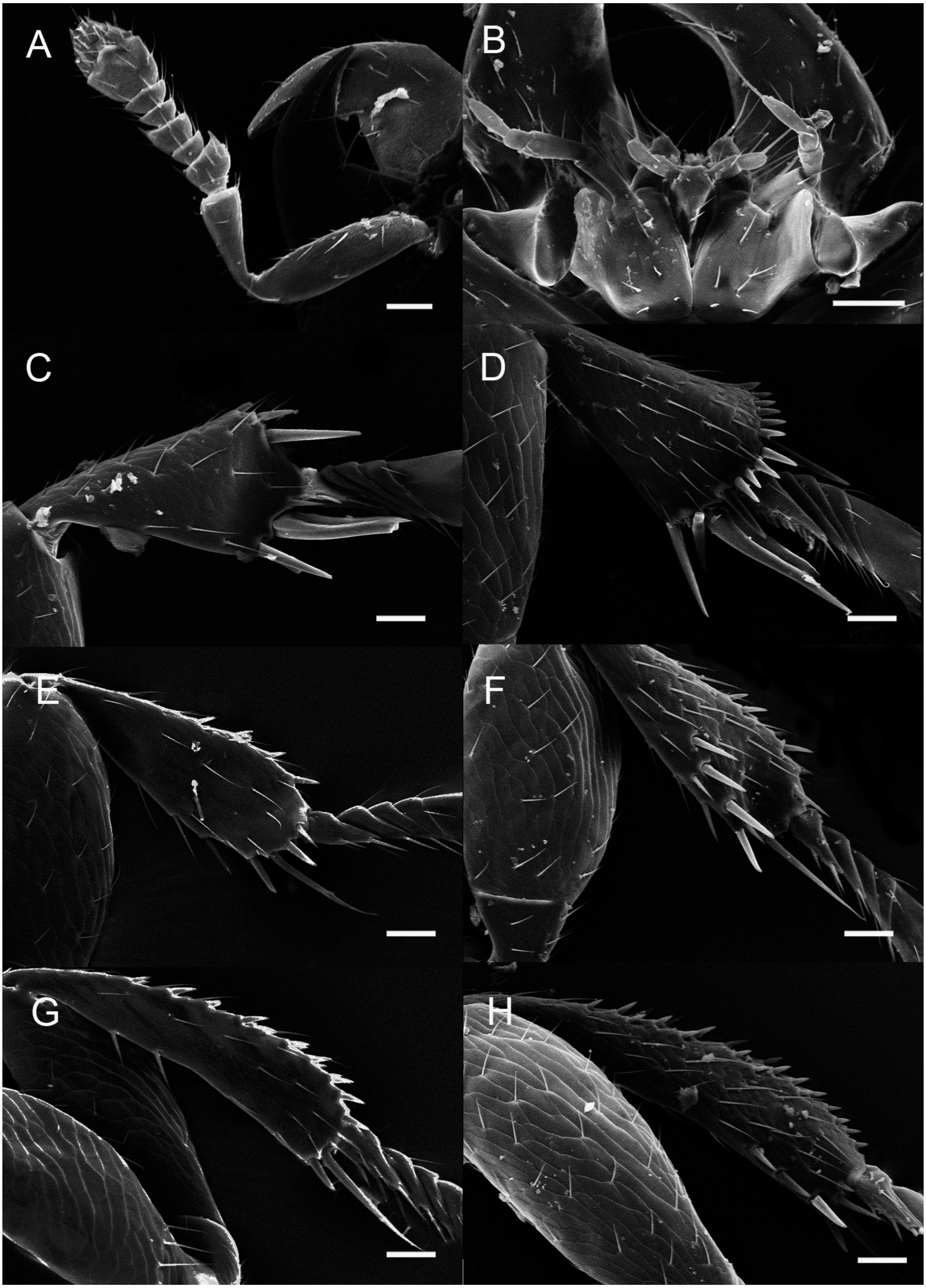

Fig. 8. Scanning electron images of male *Sycoscapter piceoscapus* sp. nov. A, Antenna; B, Maxillary palps and labial palps; C, Left fore tibia, axial; D, Right tibia, antiaxial; E, Left mid tibia, axial; F, Right mid tibia, antiaxial; G, Right hind tibia, axial; H, Left hind tibia, antiaxial. Scale bar = 0.03 mm.

Hind leg L = 0.96 mm; length ratio of coxa, trochanter, femur, tibia and tarsus = 4:1:3:3:2 (Fig. 6O). Hind tibia with a straight spur reaching the third tarsomere; 15–17 spines in axial view and 23–25 spines in antiaxial view (Fig. 8G, 8H). Hind tarsus 5-segmented, length ratio of each segment = 1:1:1:1:4.

Metasoma: Abdomen L = 0.44 mm.

Host: *Ficus microcarpa* L. f. and *Ficus benjamina* L.

Distubution: Taiwan: Hsinchu, Taichung, Changhua, Kinmen; China: Guangdong, Hainan.

Etymology: This species is named after the dark coloration of the scape in females.

Diagnosis: This species is similar to *S. benjaminae* Pramanik and Dey but can be distinguished by the characters in female including vertex shape (concave in *S. piceoscapus* vs. straight in *S. benjaminae*), scape coloration (black in *S. piceoscapus* vs. yellow in *S. benjaminae*), sculpture on antennal scrobe (reticulate in *S. piceoscapus* vs. psilate in *S. benjaminae*); in male including the ratio of rudimentary wing vestige L to mesosoma L (1.39 in *S. piceoscapus* vs. 1.7 in *S. benjaminae*).

Remarks: This species has the same hosts as *S. gajimaru*, and may co-occur in the same tree with *S. gajimaru*.

Sycoscapter monticola **Chou & Tzeng sp. nov.**

(Figs. 9, 10, 11)
urn:lsid:zoobank.org:act:5FC6CCEC-2A06-458A-956B-D4639EB3CB75

Type locality: Zhiben Forest Road, Taitung, Taiwan.

Material examined: Holotype: 1♀, Zhiben Forest Road (22.783507, 120.015736), Taitung, ex *Ficus nervosa* Heyne ex Roth., 10-V-2021, leg. P. A. Chou (NCHU). Paratypes: 1♂, Zhiben Forest Road (22.783507, 120.015736), Taitung, ex *Ficus nervosa* Heyne ex Roth., 10-V-2021, leg. P. A. Chou (NCHU); 1♂1♀, Qidu (25.122708, 121.662235), Keelung, ex *Ficus nervosa* Heyne ex Roth., 19-IX-2022, leg. P. A. Chou (TARI). Others: **Taiwan**: 1♂1♀, Urai (24.856259, 121.553437), New Taipei City, ex *Ficus nervosa* Heyne ex Roth., 11-XII-2019, leg. P. A. Chou (NCHU); 1♂1♀, Nan'ao (24.457640, 121.813020), Yilan, ex *Ficus nervosa* Heyne ex Roth., 26-III-2023, leg. P. A. Chou (NCHU). **China**: 5♀, Bawangling (19.099, 109.176), Hainan Prov., ex *Ficus nervosa* Heyne ex Roth., 11-IV-2007, col. G. Feng, W. Li, H. Y. Hu, L. M. Niu (CAS) (examined from online photographs).

Description: Female: Whole L = 5.23–5.54 mm with body L = 1.40–1.42 mm and ovipositor sheath L = 3.83–4.12 mm. Body metallic green (Fig. 9C). Compound eyes pale red (Fig. 9A). Antenna black except for the basal part of scape yellow (Fig. 9I). Legs yellow (Fig. 9J, 9L, 9N) except for the basal part of hind coxa black in antiaxial view (Fig. 9N).

Head: Obcordate in front view (Fig. 9A); H = 0.27 mm; W over compound eyes = 0.34 mm; W between compound eyes = 0.23 mm. Compound eye H 1.24× malar space L, and 2.98× compound eyes W. POL 4.84× OOL. Clypeus margin with a blunt projection in the middle (Fig. 10A). Face with raised reticulation but antennal scrobes psilate (Fig. 9A). Mandible bidentate (Fig. 9G). Maxillary palp 3-segmented, length ratio of others = 2:2:5 (Fig. 10B). Labial palp 2-segmented, length ratio = 3:2 (Fig. 10B). The distance between toruli 0.18× clypeus margin. Antennal formula 11253 and L = 0.50 mm; length ratio of scape, pedicel, anelli, funicle and clava = 14:4:1:20:10 (Fig. 9I). Scape L 4.43× W, with sparse trichoid sensillae (Fig. 10C). Pedicel L 1.55× W, with sparse trichoid sensillae (Fig. 10C). Both anelli equal in length and the second one wider (Fig. 10C). All funicular segments equal in length; the first funicular segment L 1.09× W, with 3 multiporous placoid sensillae and 5 chaetica sensillae in antiaxial view; the chaetica sensilla longer than the funicular segment (Fig. 10C). Claval segments W almost equal to funicular segments, the first claval segment L 0.87× W, with 3 multiporous placoid sensillae and 5 chaetica sensillae in antiaxial view.

Mesosoma: Mesosoma L = 0.47 mm, W = 0.31 mm; length ratio of pronotum, scutum, scutellum and propodeum = 2:3:4:1. Pronotum, scutum and scutellum with raised reticulation but propodeum psilate in dorsal view (Fig. 9B) Pronotum with collar in ventral view. Scutum with incomplete notauli (Fig. 9B). Scutellum nearly as wide as long, punctures of reticulation lengthened longitudinally (Fig. 10D). Metanotum strongly compressed and the middle covered by scutellum. Propodeum with two longitudinal keels. Forewing L = 1.09 mm, W = 0.51 mm, with 4-11 setae below the marginal vein; length ratio of submarginal vein, marginal vein, postmarginal vein and stigmal vein = 5:3:4:2 (Fig. 9P). Hind wing L = 0.70 mm, W = 0.18 mm; length ratio of submarginal vein and marginal vein = 2:3. Foreleg L = 0.76 mm; length ratio of coxa, trochanter, femur, tibia and tarsus = 3:2:5:4:3 (Fig. 9J). Fore tibia with a curve, bidentate spur reaching the apex of first tarsomere; 2-3 spines beside spur in axial view and 1 spine in antiaxial views (Fig. 10E, 10F). Fore tarsus 5-segmented, length ratio of each segment = 4:3:3:2:7. Mid leg L = 0.80 mm; length ratio of coxa, trochanter, femur, tibia and tarsus = 1:1:3:4:3 (Fig. 9L). Mid tibia with a straight spur; spur L 0.5× the first tarsomere L; 1 spine beside spur in axial view and 1 spine in antiaxial view (Fig. 10G, 10H). Mid tarsus 5-segmented, length ratio of each segment = 6:4:3:2:5. Hind leg L = 1.05 mm; length ratio of coxa, trochanter, femur, tibia and tarsus = 3:1:4:5:3 (Fig. 9N). Hind tibia with a straight spur; spur L 0.5× the first tarsomere L; 23-30 teeth in axial view and 2 spines beside spur in antiaxial view (Fig. 10I, 10J). Hind tarsus 5-segmented, length ratio of each segment = 9:4:3:2:5.

Metasoma: Abdomen without ovipositor sheath L = 0.63 mm.

Male: L = 1.57–1.70 mm. Body brown (Fig. 9D). Eyes black (Fig. 9E). Mandible dark brown (Fig. 9H). Antenna pale yellow (Fig. 9E). Legs brown (Fig. 9K, 9M, 9O).

Head: Subhexagonal in dorsal view (Fig. 9E). L without mandible = 0.50 mm; W = 0.60 mm. Mandible L = 0.31 mm, W = 0.15 mm. Mandible falcate with a fine tooth at the middle (Fig 9H). Clypeus margin concave in the middle. Maxillary palp 4-segmented, length ratio = 2:2:1:2 (Fig. 11B). Labial palp 2-segmented, length ratio= 3:1 (Fig 11B). Compound eye L 3× W. Malar space L 1.14× compound eye L. Toruli close to clypeus margin, with a ridge in the middle. Antennal formula 11153 and L = 0.39 mm; length ratio of scape, pedicel, anellus, funicle and clava = 11:7:1:8:7. Scape L 4.45× W, with sparse trichoid sensillae (Fig. 11A). Pedicel L 3.89× W, with sparse trichoid sensillae (Fig. 11A). The first and third funicular segments swollen, L 0.63× W; all funicular segments with trichoid sensillae (Fig. 11A). Claval segments as wide as the swollen segments; the first claval segment L 0.71× W, with trichoid sensillae and multiporus placoid sensillae (Fig. 11A).

Mesosoma: Oblong in dorsal view (Fig. 9F); L = 0.63 mm, W = 0.45 mm; length ratio of pronotum and the fused tergum = 3:2. Pronotum with collar in ventral view. Mesonotum, metanotum and propodeum fused in dorsal view (Fig. 9F). Rudimentary wing vestige present, L = 0.44 mm (Fig. 9F). Foreleg L = 0.92 mm; length ratio of coxa, trochanter, femur, tibia and tarsus = 3:1:2:2:2 (Fig. 9K). Fore tibia with a slightly curve, bidentate spur reaching the last tarsomere; 6 spines in axial view and 13–14 spines in antiaxial view (Fig. 11C, 11D). Fore tarsus 5-segmented, length ratio of each segment = 2:1:1:2:12. Mid leg L = 0.82 mm; length ratio of coxa, trochanter, femur, tibia and tarsus = 2:1:2:2:2 (Fig. 9M). Mid tibia with a straight spur reaching the second tarsomere; 14–15 spines in axial view and 13–16 spines in antiaxial view (Fig. 11E, 11F). Mid tarsus 5-segmented, length ratio of each segment = 2:1:1:1:6. Hind leg L = 1.17 mm; length ratio of coxa, trochanter, femur, tibia and tarsus = 7:2:5:6:4 (Fig. 9O). Hind tibia with a straight spur reaching the third tarsomere; 18–20 spines in axial view and 23 spines in antiaxial view (Fig. 11G, 11H). Hind tarsus 5-segmented, length ratio of each segment = 1:1:1:1:6.

Metasoma: Abdomen L = 0.67 mm.

Host: *Ficus nervosa* Heyne ex Roth.

Distubution: Taiwan: Keelung, New Taipei, Yilan, Taitung; China: Hainan.

Etymology: This species is named after the mountain habitat of its host fig tree.

Diagnosis: This species has a subhexagonal head shape in males that shows no similarity with any other described species.

Remarks: This species utilizes shares the same host species with an Indian congener, *S. vijayaii* Priyadasanan, but the two species can be distinguished by the characters in female including the ratio of POL to OOL (4.84 in *S. monticola* vs. 11 in *S. vijayaii*), the ratio of ovipositor L to metasoma L (6.08 in *S. monticola* vs. 7 in *S. vujayaii*); in male including the head shape (subhexagonal in *S. monticola* vs. rectangular in *S. vijayaii*), the claval segments (3 in *S. monticola* vs. 2 in *S. vijayaii*).

***Sycoscapter ishiianus* Chou & Tzeng sp. nov.**

(Figs. 12, 13, 14)
urn:lsid:zoobank.org:act:E98F9E4A-0B39-4683-84D5-26F485590FFD

Type locality: South Dist., Taichung, Taiwan.

Material examined: Holotype: 1♀, South Dist. (24.128055, 120.678623), Taichung City, ex *Ficus subpisocarpa* Gagnep., 31-VII-2023, leg. P. A. Chou (NCHU). Paratypes: 1♂, South Dist. (24.128055, 120.678623), Taichung City, ex *Ficus subpisocarpa* Gagnep., 31-VII-2023, leg. P. A. Chou (NCHU); 1♂1♀, Shuangliu (22.217694, 120.803907), Pingtung, ex *Ficus subpisocarpa* Gagnep., 8-II-2021, leg. C. Y. Huang (TARI). Others: **Taiwan**: 1♂1♀, Lover's Lake Park (25.156796, 121.705576), Keelung, ex *Ficus subpisocarpa* Gagnep., 24-XI-2020, leg. P. A. Chou (NCHU); 1♂1♀, Tianmu (25.118908, 121.532423), Taipei City, ex *Ficus subpisocarpa* Gagnep., 19-VI-2022, leg. Y. R. Fang (NCHU); 1♂1♀, Shen'ao (25.127480, 121.816726), New Taipei City, ex *Ficus subpisocarpa* Gagnep., 19-VIII-2022, leg. P. A. Chou (NCHU); 1♂1♀, Anping (22.995227, 120.164240), Tainan, ex *Ficus subpisocarpa* Gagnep., 2-IX-2018, leg. P. A. Chou (NCHU); 1♂1♀, Frog Rock Trail (21.942526, 120.799618), Pingtung, ex *Ficus subpisocarpa* Gagnep., 24-XI-2020, leg. P. A. Chou (NCHU); 1♂1♀, Carp Mountain Park (22.753445, 121.144535), Taitung, ex *Ficus subpisocarpa* Gagnep., 2-IX-2022, leg. P. A. Chou (NCHU); 1♂1♀, Penghu Visitor Center (23.557232, 119.608105), Penghu, ex *Ficus subpisocarpa* Gagnep., 3-VI-2019, leg. P. A. Chou (NCHU); 1♂1♀, Kinhu Junior High

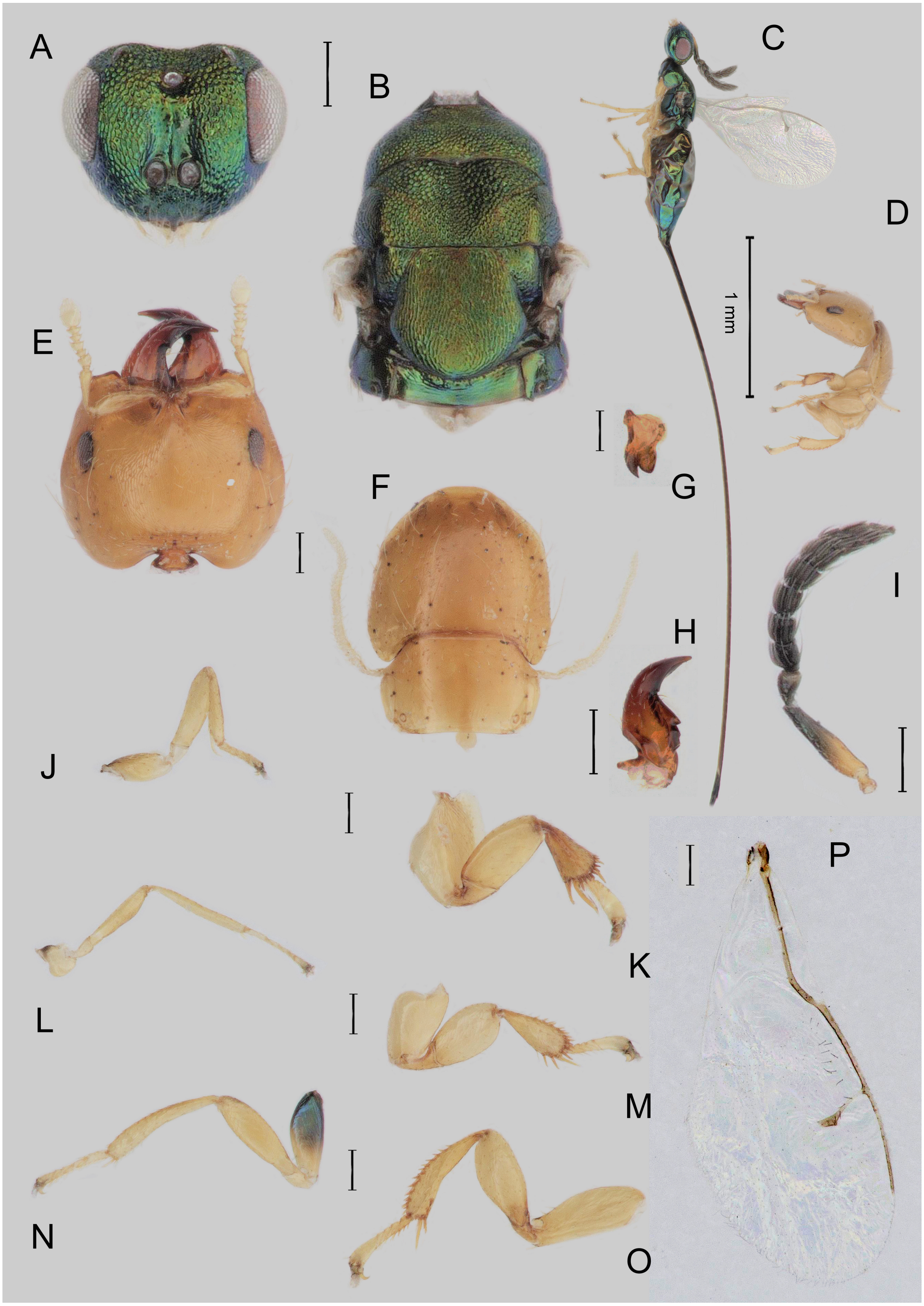

Fig. 9. *Sycoscapter monticola* sp. nov. A, Female head, front; B, Female mesosoma, dorsal; C, Female habitus, lateral; D, Male habitus, lateral; E, Male head, dorsal; F, Male mesosoma, dorsal; G, Female left mandible, ventral; H, Male left mandible, dorsal; I, Female antenna; J, Female right foreleg; K, Male right foreleg; L, Female right mid leg; M, Male right mid leg; N, Female right hind leg; O, Male right hind leg; P, Female forewing. Scale bar = 0.1 mm if no number is noted.

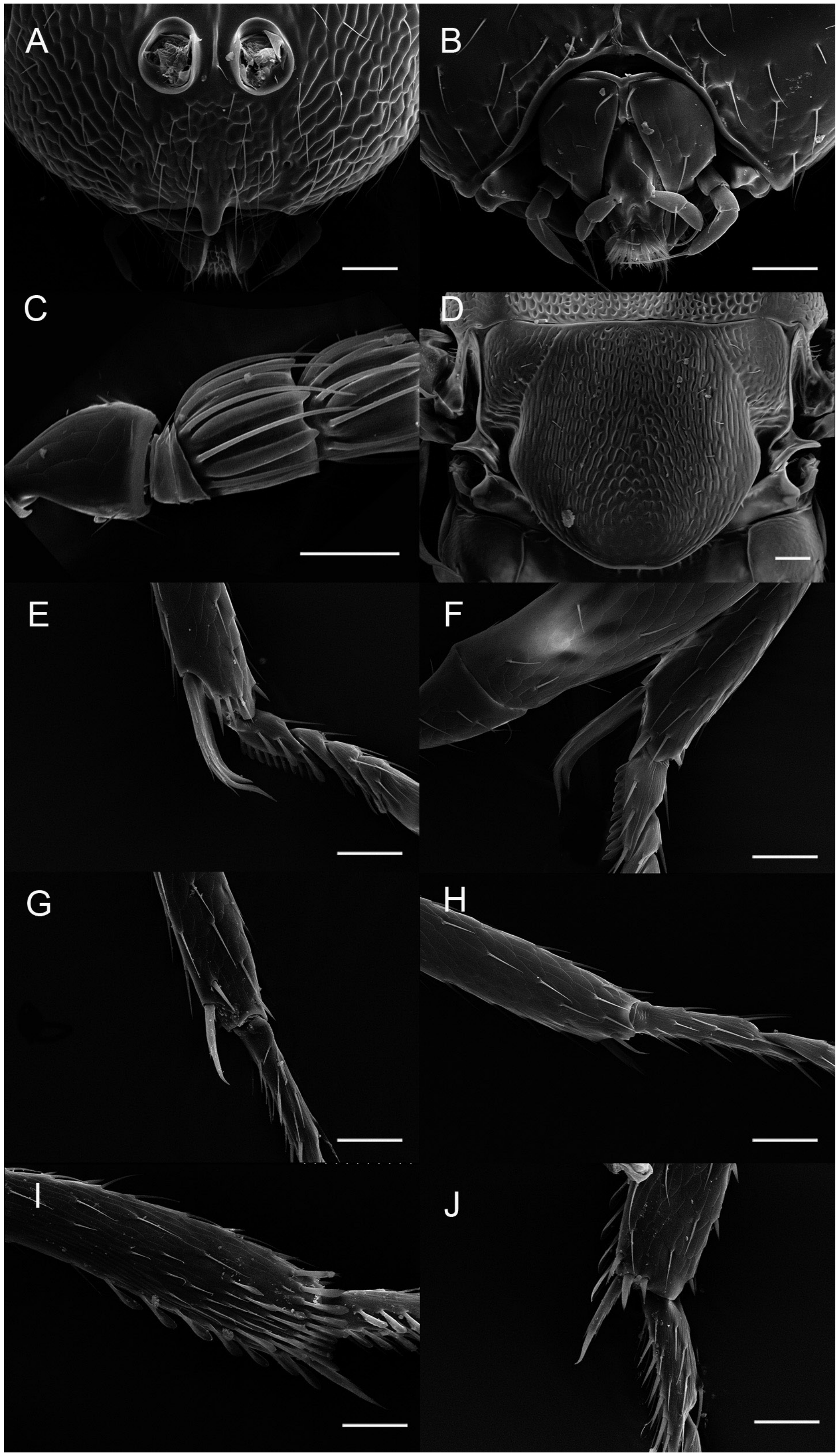

Fig. 10. Scanning electron images of female *Sycoscapter monticola* sp. nov. A, Toruli and epistomal margin; B, Maxillary palps and labial palps; C, Anelli and the first funiculus; D, Scutellum; E, Left fore tibia, axial; F, Right tibia, antiaxial; G, Left mid tibia, axial; H, Right mid tibia, antiaxial; I, Right hind tibia, axial; J, Left hind tibia, antiaxial. Scale bar = 0.03 mm.

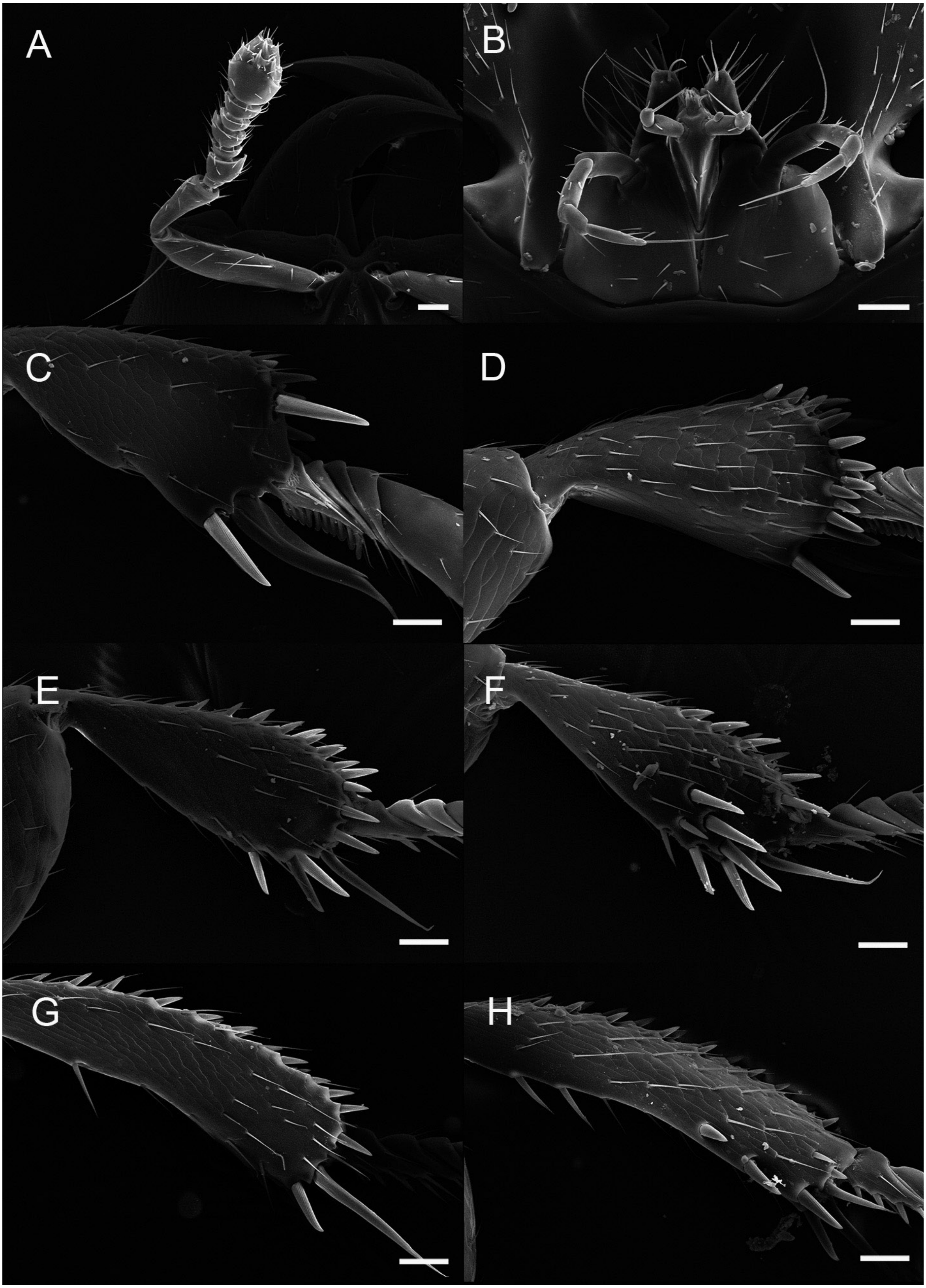

Fig. 11. Scanning electron images of male *Sycoscapter monticola* sp. nov. A, Antenna; B, Maxillary palps and labial palps; C, Left fore tibia, axial; D, Right tibia, antiaxial; E, Left mid tibia, axial; F, Right mid tibia, antiaxial; G, Right hind tibia, axial; H, Left hind tibia, antiaxial. Scale bar = 0.03 mm.

School (24.437888, 118.420643), Kinmen, ex *Ficus subpisocarpa* Gagnep., 23-X-2021, leg. P. A. Chou (NCHU); **Japan**: 1♂1♀, Iriomote (24.384750, 123.893395), Okinawa, ex *Ficus subpisocarpa* Gagnep., 8-VII-2018, leg. P. A. Chou (NCHU).

Description: Female: Whole L = 4.43–4.65 mm with body L = 1.22–1.24 mm and ovipositor sheath L = 3.19–3.41 mm. Body metallic green (Fig. 12C). Compound eyes pale red (Fig. 12A). Antenna black except for the yellow basal part of the scape (Fig. 12I). Legs yellow (Fig. 12J, 12L, 12N); basal part of hind coxa and middle of hind femur black in antiaxial view (Fig. 12N).

Head: Obcordate in front view (Fig. 12A). H = 0.26 mm, W over compound eyes = 0.37 mm; W between compound eyes = 0.21 mm. Compound eye H 1.47× malar space L, and 2.44× compound eyes W. POL 4.95× OOL. Clypeus margin with a blunt projection in the middle (Fig. 13A). Face with raised reticulation but antennal scrobes psilate (Fig. 12A). Mandible bidentate (Fig. 12G). Maxillary palp 3-segmented, length ratio = 3:4:5 (Fig. 13B). Labial palp 2-segmented, length ratio = 3:2 (Fig. 13B). The distance between toruli 0.3× clypeus margin. Antennal formula 11253 and L = 0.55 mm; length ratio of scape, pedicel, anelli, funicle and clava = 14:4:1:20:10 (Fig. 12I). Scape L 4.57× W, with sparse trichoid sensillae (Fig. 13C). Pedicel L 1.08× W, with sparse trichoid sensillae (Fig. 13C). Both anelli equal in length and the second one wider (Fig. 13C). All funicular segments equal in length; the first funicular segment L 0.98× W, with 3 multiporous placoid sensillae and 7 chaetica sensillae in antiaxial view; the chaetica sensilla longer than the funicular segment (Fig. 13C). Claval segments slightly wider than funicular segments; the first claval segment L 0.89× W, with 3 multiporous placoid sensillae and 7 chaetica sensillae in antiaxial view.

Mesosoma: Mesosoma L = 0.46 mm, W = 0.36 mm, length ratio of pronotum, scutum, scutellum and propodeum = 2:4:6:1. Pronotum, scutum and scutellum with raised reticulation but propodeum psilate in dorsal view (Fig. 12B). Pronotum with collar in ventral view. Scutum with incomplete notauli (Fig. 12B). Scutellum nearly as wide as long, punctures of reticulation lengthened longitudinally (Fig. 13D). Metanotum strongly compressed and the middle covered by scutellum. Propodeum with two longitudinal keels. Forewing L = 1.19 mm, W = 0.53 mm, with 9–13 setae below the marginal vein; length ratio of submarginal vein, marginal vein, postmarginal vein and stigmal vein = 5:3:4:2 (Fig. 12P). Hind wing L = 0.80 mm, W = 0.16 mm; length ratio of submarginal vein and marginal vein = 2:3. Foreleg L = 0.75 mm; length ratio of coxa, trochanter, femur, tibia and tarsus = 3:2:5:4:3 (Fig. 12J). Fore tibia with a curve, bidentate spur reaching the apex of first tarsomere; 2 spines beside spur in axial view and 1 spine in antiaxial views (Fig. 13E, 13F). Fore tarsus 5-segmented, length ratio of each segment = 4:3:3:2:7. Mid leg L = 0.81 mm; length ratio of coxa, trochanter, femur, tibia and tarsus = 1:1:3:4:3 (Fig. 12L). Mid tibia with a straight spur; spur L 0.5× the first tarsomere L; 2 spines beside spur in axial view but 2 spines in antiaxial view (Fig. 13G, 13H). Mid tarsus 5-segmented, length ratio of each segment = 7:4:3:2:4. Hind leg L = 1.04 mm; length ratio of coxa, trochanter, femur, tibia and tarsus = 3:1:3:4:3 (Fig. 12N). Hind tibia with a straight spur; spur L 0.5× the first tarsomere L; 23–25 teeth in axial view and 2 spines beside spur in antiaxial view (Fig. 13I, 13J). Hind tarsus 5-segmented, length ratio of each segment = 6:4:3:2:5.

Metasoma: Abdomen without ovipositor sheath L = 0.73 mm.

Male: L = 1.69–1.75 mm. Body brown (Fig. 12D). Eyes black (Fig. 12E). Mandible dark brown (Fig. 12H). Antenna pale yellow (Fig. 12E). Legs brown (Fig. 12K, 12M, 12O).

Head: Long rectangular in dorsal view (Fig. 12E). L without mandible = 0.43 mm, W = 0.39 mm. Mandible L = 0.28 mm, W = 0.15 mm. Mandible falcate with a fine tooth at the middle (Fig 12H). Clypeus margin concave in the middle. Maxillary palp 4-segmented, length ratio = 3:2:1:2 (Fig. 14B). Labial palp 2-segmented, length ratio = 3:1 (Fig 14B). Compound eye L 3× W. Malar space L 1.73× compound eye L. Toruli close to clypeus margin, with a ridge in the middle. Antennal formula 11153 and L = 0.39 mm; length ratio of scape, pedicel, anelli, funicle and clava = 14:7:1:8:6. Scape L 4.76× W, with sparse trichoid sensillae (Fig. 14A). Pedicel L 3.7× W, with sparse trichoid sensillae (Fig. 14A). The first and third funicular segments swollen, L 0.81× W; other funicular segments L 0.88× W; all funicular segments with trichoid sensillae (Fig. 14A). Claval segments wider than the swollen funicular segments; the first claval segment L 1.03× W, with trichoid sensillae and multiporus placoid sensillae (Fig. 14A).

Mesosoma: Subpentagon in dorsal view (Fig. 12F). L = 0.51 mm, W = 0.36 mm; length ratio of pronotum and the fused tergum = 3:2 Pronotum with collar in ventral view. Mesonotum, metanotum and propodeum fused in dorsal view (Fig. 12F). Rudimentary wing vestige present, L = 0.33 mm (Fig. 12F). Foreleg L = 0.91 mm; length ratio of coxa, trochanter, femur, tibia and tarsus = 3:1:4:2:2 (Fig. 12K). Fore tibia with a slightly curve, bidentate spur reaching the fourth tarsomere; 7 spines in axial view and 8 spines in antiaxial view (Fig. 14C, 14D). Fore tarsus 5-segmented, length ratio of each segment = 1:1:1:1:5.

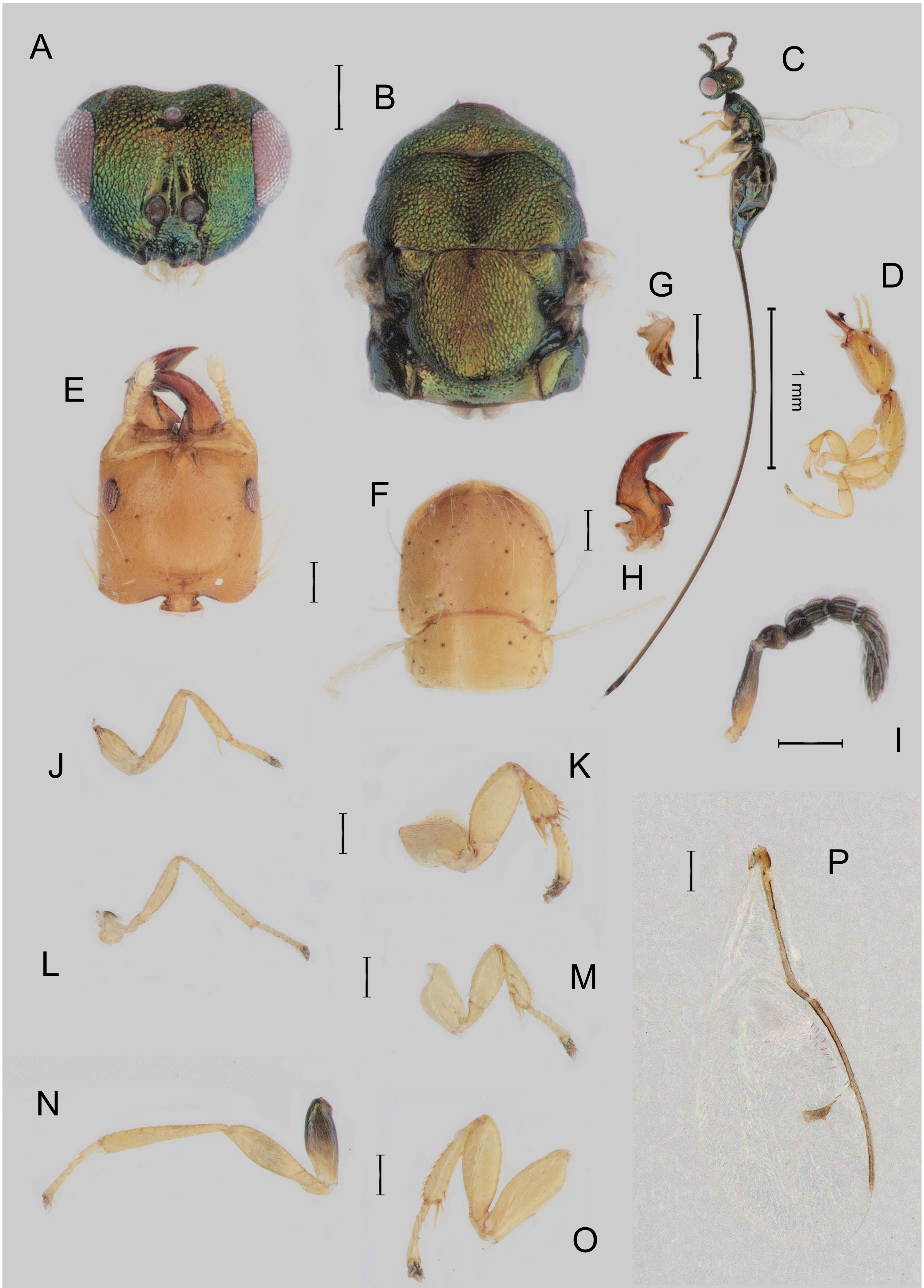

Fig. 12. *Sycoscapter ishiianus* sp. nov. A, Female head, front; B, Female mesosoma, dorsal; C, Female habitus, lateral; D, Male habitus, lateral; E, Male head, dorsal; F, Male mesosoma, dorsal; G, Female left mandible, ventral; H, Male left mandible, dorsal; I, Female antenna; J, Female right foreleg; K, Male right foreleg; L, Female right mid leg; M, Male right mid leg; N, Female right hind leg; O, Male right hind leg; P, Female forewing. Scale bar = 0.1 mm if no number is noted.

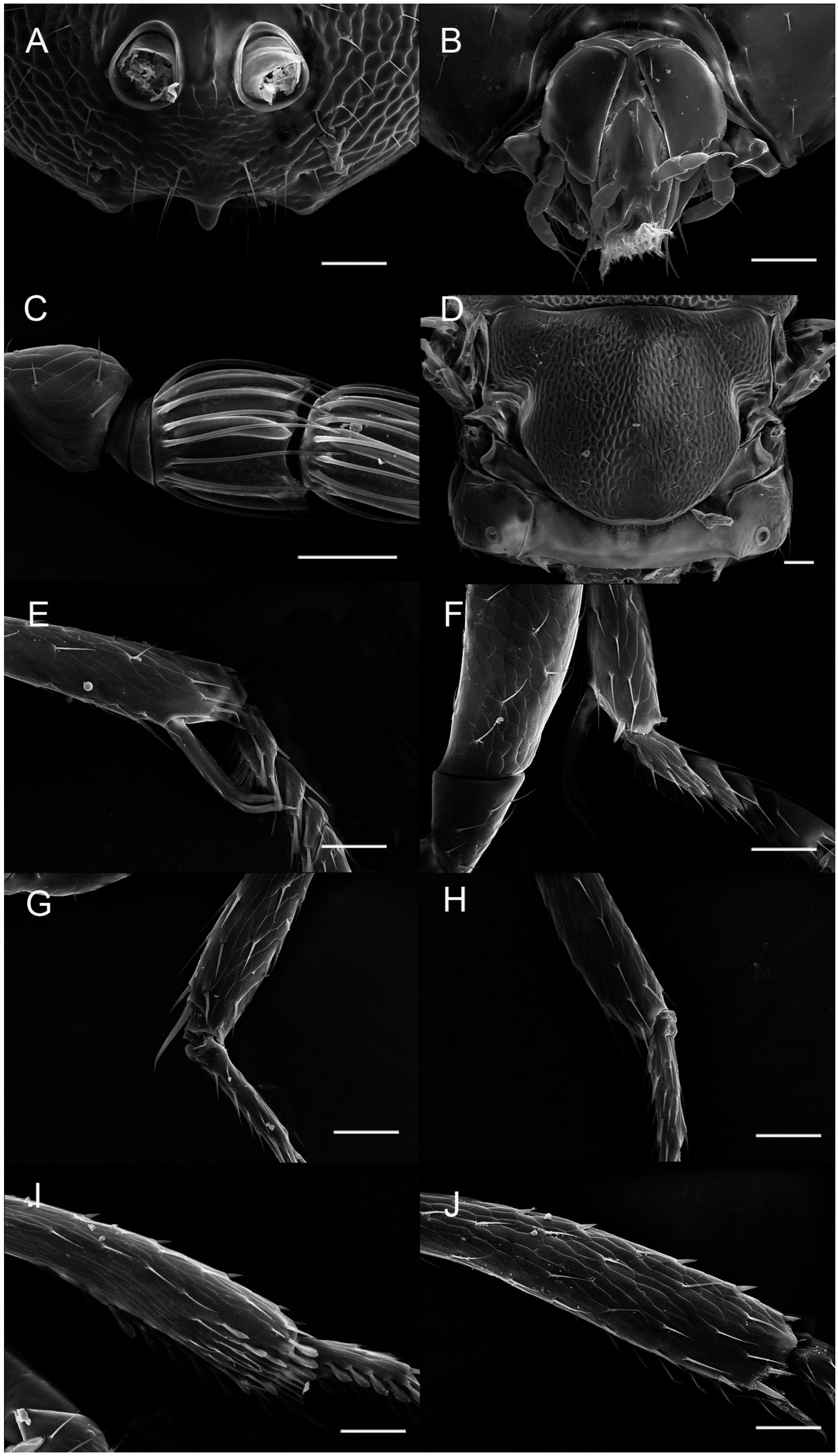

Fig. 13. Scanning electron images of female *Sycoscapter ishiiaus* sp. nov. A, Toruli and epistomal margin; B, Maxillary palps and labial palps; C, Anelli and the first funiculus; D, Scutellum; E, Left fore tibia, axial; F, Right tibia, antiaxial; G, Left mid tibia, axial; H, Right mid tibia, antiaxial; I, Right hind tibia, axial; J, Left hind tibia, antiaxial. Scale bar = 0.03 mm.

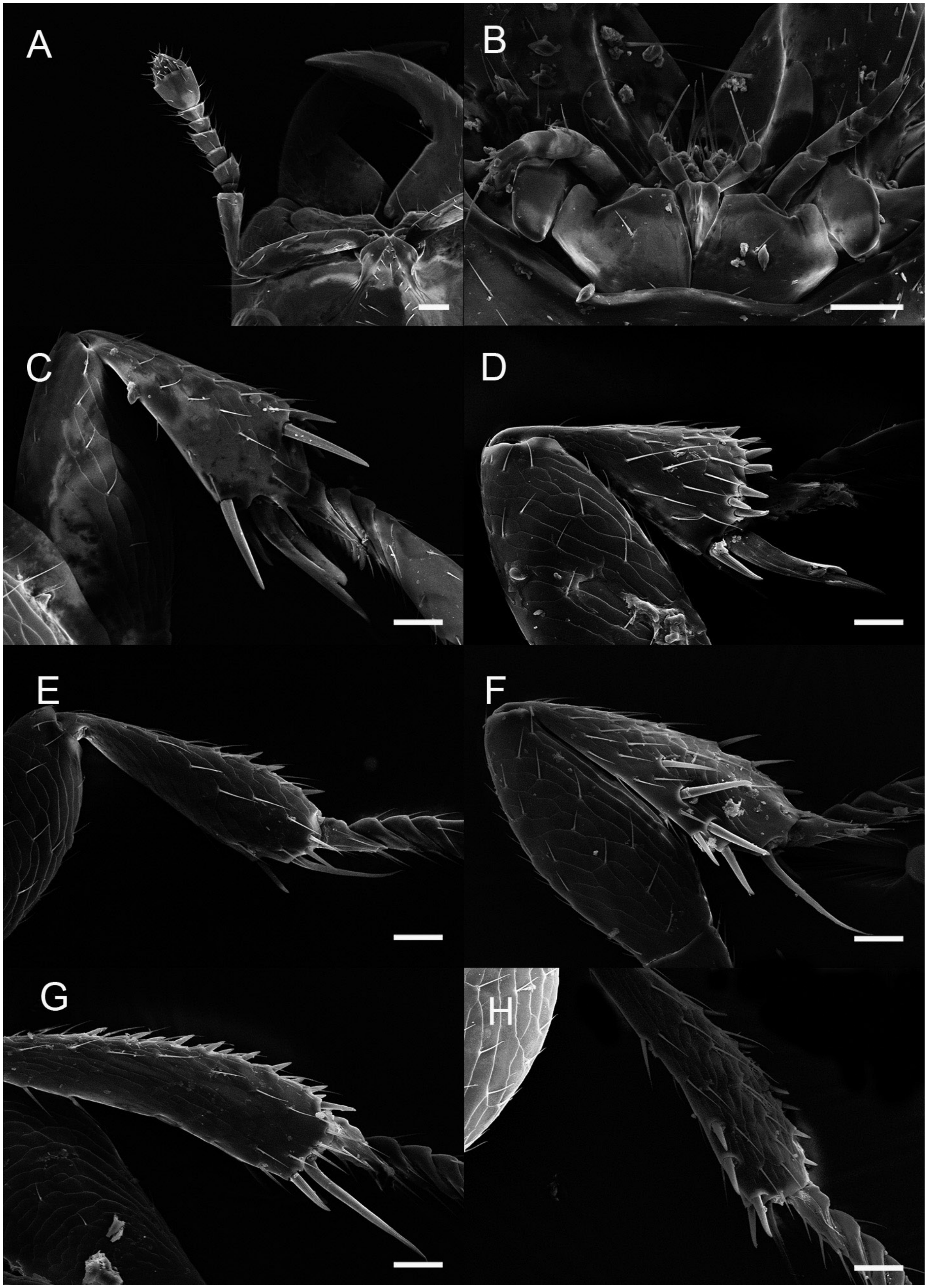

Fig. 14. Scanning electron images of male *Sycoscapter ishiianus* sp. nov. A, Antenna; B, Maxillary palps and labial palps; C, Left fore tibia, axial; D, Right tibia, antiaxial; E, Left mid tibia, axial; F, Right mid tibia, antiaxial; G, Right hind tibia, axial; H, Left hind tibia, antiaxial. Scale bar = 0.03 mm.

Mid leg L = 0.83 mm; length ratio of coxa, trochanter, femur, tibia and tarsus = 2:1:2:2:2 (Fig. 12M). Mid tibia with a straight spur reaching the second tarsomere; 6–9 spines in axial view and 7–8 spines in antiaxial view (Fig. 14E, 14F). Mid tarsus 5-segmented, length ratio of each segment = 1:1:1:1:5. Hind leg L = 1.02 mm; length ratio of coxa, trochanter, femur, tibia and tarsus = 4:1:3:3:3 (Fig. 12O). Hind tibia with a straight spur reaching the third tarsomere; 10–13 spines in axial view and 8–11 spines in antiaxial view (Fig. 14G, 14H). Hind tarsus 5-segmented, length ratio of each segment = 1:1:1:1:5.

Metasoma: Abdomen L = 0.47 mm.

Host: *Ficus subpisocarpa* Gagnep.

Distribution: Taiwan: Keelung, Taipei, New Taipei, Taichung, Tainan, Pingtung, Taitung, Penghu, Kinmen; Japan: Iriomote island.

Etymology: This species is named in honor of Tei Ishii, who contributed greatly to fig wasp taxonomy in East Asia.

Diagnosis: This species is similar to *S. infectorius* but can be distinguished from the characters in female including the ratio of ovipositor L to metasoma L (4.37 in *S. ishiianus* vs. 5.6 in *S. infectorius*), the maxillary palp segment (four in *S. ishiianus* vs, three in *S. infectorius*); in male including spur on fore tibia (not exceeding the last tarsomere in *S. ishiianus* vs. doing so in *S. infectorius*).

Sycoscapter littoralis **Chou & Tzeng sp. nov.**

(Figs. 15, 16, 17)
urn:lsid:zoobank.org:act:64C41C6C-F6CB-4F84-8C10-857B3D093D7E

Type locality: Dawu, Taitung, Taiwan.

Material examined: Holotype: 1♀, Dawu (22.309822, 120.889147), Taitung, ex *Ficus caulocarpa* (Miq.) Miq., 3-IX-2022, leg. P. A. Chou (NCHU). Paratypes: 1♂, Dawu (22.309822, 120.889147), Taitung, ex *Ficus caulocarpa* (Miq.) Miq., 3-IX-2022, leg. P. A. Chou (NCHU); 1♂1♀, Shen'ao (25.128355, 121.813439), New Taipei City, ex *Ficus caulocarpa* (Miq.) Miq., 2-X-2022, leg. P. A. Chou (TARI). Others: 1♂1♀, Taitung Seashore Park (22.751577, 121.161233), Taitung, ex *Ficus caulocarpa* (Miq.) Miq., 2-IX-2022, leg. P. A. Chou (NCHU); 1♂1♀, Kenting Forest Recreation Park (21.963324, 120.812599), Pintong, ex *Ficus caulocarpa* (Miq.) Miq., 19-IV-2023, leg. P. A. Chou (NCHU); 1♂1♀, Lanyu (22.035262, 121.563452), Taitung, ex *Ficus caulocarpa* (Miq.) Miq., 4-X-2020, leg. P. A. Chou (NCHU).

Description: **Female**: Whole L = 2.99–3.25 mm with body L = 0.93–1.03 mm and ovipositor sheath L = 2.06–2.22 mm. Body metallic green (Fig. 15C). Compound eyes pale red (Fig. 15A). Antenna black except for the yellow basal part of the scape (Fig. 15I). Legs yellow (Fig. 15J, 15L, 15N); middle of hind femur slightly black (Fig. 15L); basal part of hind coxa and middle of hind femur black in antiaxial view (Fig. 15N).

Head: Rounded in front view (15A). H = 0.24 mm, W over compound eyes = 0.28 mm; W between compound eyes = 0.19 mm. Compound eye H 1.41× malar space, and 3.05× compound eyes W. POL 3.12× OOL. Clypeus margin with a blunt projection in the middle (Fig. 16A). Face with raised reticulation but antennal scrobes psilate (Fig. 15A). Mandible bidentate (Fig. 15G). Maxillary palp 3-segmented, length ratio of others = 2:4:3 (Fig. 16B). Labial palp 2-segmented, length ratio = 3:2 (Fig. 16B). The distance between toruli 0.27× clypeus margin. Antennal formula 11253 and L = 0.36 mm; length ratio of scape, pedicel, anelli, funicle and clava = 14:4:1:20:10 (Fig. 15I). Scape L 4× W, with sparse trichoid sensillae (Fig. 16C). Pedicel L 1.25× W, with sparse trichoid sensillae (Fig. 16C). Both anelli equal in length and the second one wider (Fig. 16C). All funicular segments equal in length; the first funicular segment L 0.82× W, with 3 multiporous placoid sensillae and 3 chaetica sensillae in antiaxial view. The chaetica sensilla longer than funicular segment (Fig. 16C). Claval segments slightly wider than funicular segments; the first claval segment L 1× W, with 2 multiporous placoid sensillae and 4 chaetica sensillae in antiaxial view.

Mesosoma: Mesosoma L = 0.43 mm, W = 0.27 mm; length ratio of pronotum, scutum, scutellum and propodeum = 2:3:4:1. Pronotum, scutum and scutellum with raised reticulation but propodeum psilate in dorsal view (Fig. 15B). Pronotum with collar in ventral view. Scutum with incomplete notauli (Fig. 15B). Scutellum nearly as wide as long, punctures of reticulation lengthened longitudinally (Fig. 16D). Metanotum strongly compressed and the middle covered by scutellum. Propodeum with two longitudinal keels. Forewing L = 0.86 mm, W = 0.37 mm, with 9-10 setae below the marginal vein; length ratio of submarginal vein, marginal vein, postmarginal and stigmal vein = 5:3:4:2 (Fig. 15P). Hind wing L = 0.54 mm, W = 0.12 mm; length ratio of submarginal vein and marginal vein L = 2:3. Foreleg L = 0.57 mm; length ratio of coxa, trochanter, femur, tibia and tarsus = 3:2:5:4:3 (Fig. 15J). Fore tibia with a curve, bidentate spur reaching the first tarsomere; 2 spines beside spur in axial view and 1 spine in antiaxial views (Fig. 16E, 16F). Fore tarsus five segments, length ratio of each segment = 2:2:1:1:3. Mid leg L = 0.59 mm; length ratio of coxa, trochanter, femur, tibia and tarsus = 1:1:3:4:3 (Fig. 15L). Mid tibia with a straight spur; spur L 0.5× the first tarsomere L; 1 spine beside spur in axial view but no spine in antiaxial view

(Fig. 16G, 16H). Mid tarsus five segments, length ratio of each segment = 7:4:3:2:5. Hind leg L = 0.82 mm; length ratio of coxa, trochanter, femur, tibia and tarsus L = 3:1:3:5:3 (Fig. 15N). Hind tibia with a straight spur; spur L 0.5× the first tarsomere L; 25–27 teeth in axial view and 2 spines beside spur in antiaxial view (Fig. 16I, 16J). Hind tarsus five segments, length ratio of each segment = 7:4:3:2:5.

Metasoma: Abdomen without ovipositor sheath L = 0.59 mm.

Male: L = 1.34–1.43 mm. Body brown (Fig. 15D). Eyes black (Fig. 15E). Mandible dark brown (Fig. 15H). Antenna pale yellow (Fig. 15E). Legs brown (Fig. 15K, 15M, 15O).

Head: Long rectangular in dorsal view (Fig. 15E). L without mandible = 0.42 mm, W = 0.42 mm. Mandible L = 0.28 mm, W = 0.11 mm. Mandible falcate with a fine tooth at the middle (Fig 15H). Clypeus margin concave in the middle. Maxillary palp 4-segmented, length ratio = 3:3:1:2 (Fig. 17B). Labial palp 2-segmented, length ratio = 2:3 (Fig 17B). Compound eye L 3× W. Malar space L 1.95× compound eye L. Toruli close to clypeus margin, with a ridge in the middle. Antennal formula 11153 and L = 0.39 mm; length ratio of scape, pedicel, anellus, funicle and clava = 11:7:1:8:7. Scape L 4.36× W, with sparse trichoid sensillae (Fig. 17A). Pedicel L 2.68× W, with sparse trichoid sensillae (Fig. 17A). The first and third funicular segments swollen, L 0.8× W; other funicular segments L 0.72× W; all funicular segments with trichoid sensillae (Fig. 17A). Claval segments as wide as the swollen funicular segments; the first claval segment L 1.18× W, with trichoid sensillae and multiporus placoid sensillae (Fig. 17A).

Mesosoma: Oblong in dorsal view (Fig. 15F); L = 0.44 mm, W = 0.31 mm; length ratio of pronotum and the fused tergum = 2:1. Pronotum with collar in ventral view. Mesonotum, metanotum and propodeum fused in dorsal view (Fig. 15F). Rudimentary wing vestige present, L = 0.29 mm (Fig. 15F). Foreleg L = 1.52 mm; length ratio of coxa, trochanter, femur, tibia and tarsus = 3:1:3:2:2 (Fig. 15K). Fore tibia with a slightly curve, bidentate spur reaching the fourth tarsomere; 4–5 spines in axial view and 9–11 spines in antiaxial view (Fig. 17C, 17D). Fore tarsus 5-segmented, length ratio of each segment = 2:1:1:1:7. Mid leg L = 0.68 mm; length ratio of coxa, trochanter, femur, tibia and tarsus L = 2:1:2:2:2 (Fig. 15M). Mid tibia with a straight spur reaching the second tarsomere; 8–11 spines in axial view and 7–10 spines in antiaxial view (Fig. 17E, 17F). Mid tarsus five segments, length ratio of each segment = 1:1:1:1:5. Hind leg L = 0.90 mm; length ratio of coxa, trochanter, femur, tibia and tarsus L = 4:1:4:4:3 (Fig. 15O). Hind tibia with a straight spur reaching the third tarsomere; 7–8 spines in axial view and 15 spines in antiaxial view (Fig. 17G, 17H). Hind tarsus five segments, length ratio of each segment = 1:1:1:1:4.

Metasoma: Abdomen L = 0.38 mm.

Host: *Ficus caulocarpa* (Miq.) Miq.

Distribution: Taiwan: New Taipei, Taitung, Pintong.

Etymology: This species is named after the coastal habitats of its host fig tree.

Diagnosis: 1. This is species is similar to *S. infectorius* Joseph but can be distinguished from the characters in female including the ratio of POL to OOL (5.35 in *S. littoralis* vs. 6.7 in *S. infectorius*), the seta number on forewing (9–10 in *S. littoralis* vs. 15 in *S. infectorius*), ratio of ovipositor L to metasoma L (3.76 in *S. littoralis* vs. 5.6–6 in *S. infectorius*); in male including the spur on fore tibia (not exceeding the last tarsomere in *S. littoralis* vs. doing so in *S. infectorius*).

2. This species is also similar to *S. ishiianus* sp. nov. but can be distinguished from the characters in female including the head shape (rounded in *S. littoralis* vs. subtriangle in *S. ishiianus*), the maxillary palp segment (three in *S. littoralis* vs. four in *S. ishiianus*); in male including the pronotum shape (oblong in *S. littoralis* vs. subpentagonal in *S. ishiianus*).

Key to the *Sycoscpater* species associated with monoecious figs in Taiwan

1. Fully winged; body metallic green (Figs. 3C; 6C; 9C; 12C; 15C) .... Female, 2
- Wings reduced to filiform vestige; body yellowish brown (Figs. 3F; 6F; 9F; 12F; 15F) .... Male, 6
2. Scape all yellowish (Fig. 3I); punctures of reticulation on scutellum rounded (Fig. 4D) .... *S. gajimaru*
- Scape black with slight yellow on the basal part (Figs. 6I; 9I; 12I; 15I); punctures of reticulation on scutellum lengthened longitudinally (Figs. 7D; 10D; 13D; 16D) 3
3. POL almost 7× OOL (Fig. 6A); Scutellum L 4× pronotum L (Fig. 6B) .... *S. piceoscapus*
- POL < 5× OOL (Figs. 9A; 12A; 15A); Scutellum L 2 or 3× pronotum L (Figs. 9B; 12B; 15B) 4
4. Head H 3.5× W over compound eyes (Fig. 12A); Scutellum L 3× pronotum L (Fig. 12B) .... *S. ishiianus*
- Head H at least 4× W over compound eyes (Figs. 9A; 15A); Scutellum L 2× pronotum L (Figs. 9B; 15B) 5
5. Antennal scrobes psilate (Fig. 9A); middle part of hind femur without black spot in antiaxial view (Fig. 9N) .... *S. monticola*
- Antennal scrobes with raised reticulation (Fig. 15A); middle part of hind femur with black spot in antiaxial view (Fig. 15N) .... *S. littoralis*
6. Scape L 2.5× W (Fig. 5A); compound eye L 2.5× W (Fig. 3E) .... *S. gajimaru*
- Scape L at least 3× W (Figs. 8A; 11A; 14A; 17A); compound eye L at least 3× W (Figs. 6E; 9E; 12E; 15E) 7
7. Head long ovate (Fig. 6E); compound eye L 3.5× W (Fig. 6E) .... *S. piceoscapus*
- Head subhexagonal or long rectangular (Figs. 9E; 12E; 15E); compound eye L 3× W (Figs. 9E; 12E; 15E) 8

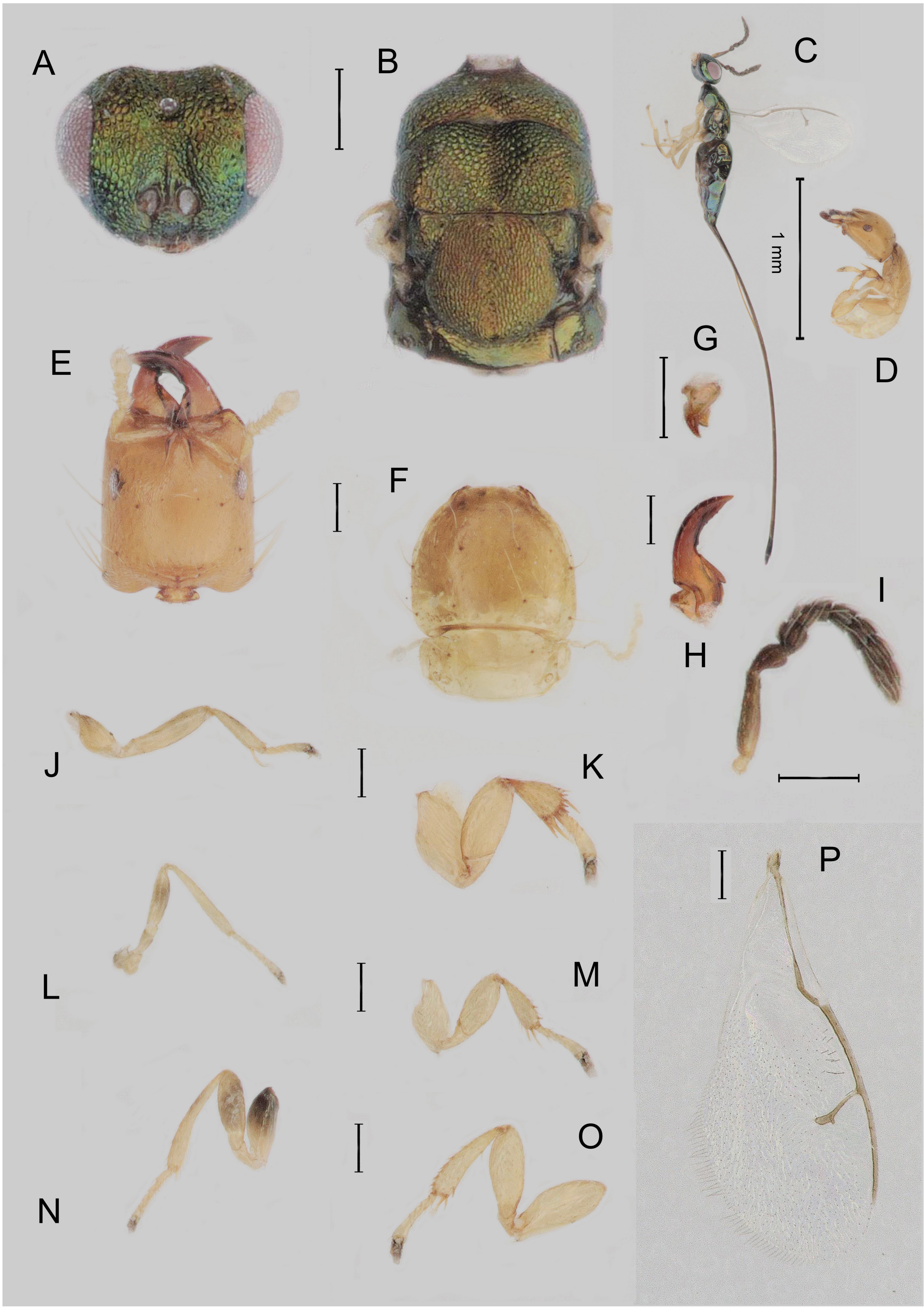

Fig. 15. *Sycoscapter littoralis* sp. nov. A, Female head, front; B, Female mesosoma, dorsal; C, Female habitus, lateral; D, Male habitus, lateral; E, Male head, dorsal; F, Male mesosoma, dorsal; G, Female left mandible, ventral; H, Male left mandible, dorsal; I, Female antenna; J, Female right foreleg; K, Male right foreleg; L, Female right mid leg; M, Male right mid leg; N, Female right hind leg; O, Male right hind leg; P, Female forewing. Scale bar = 0.1 mm if no number is noted.

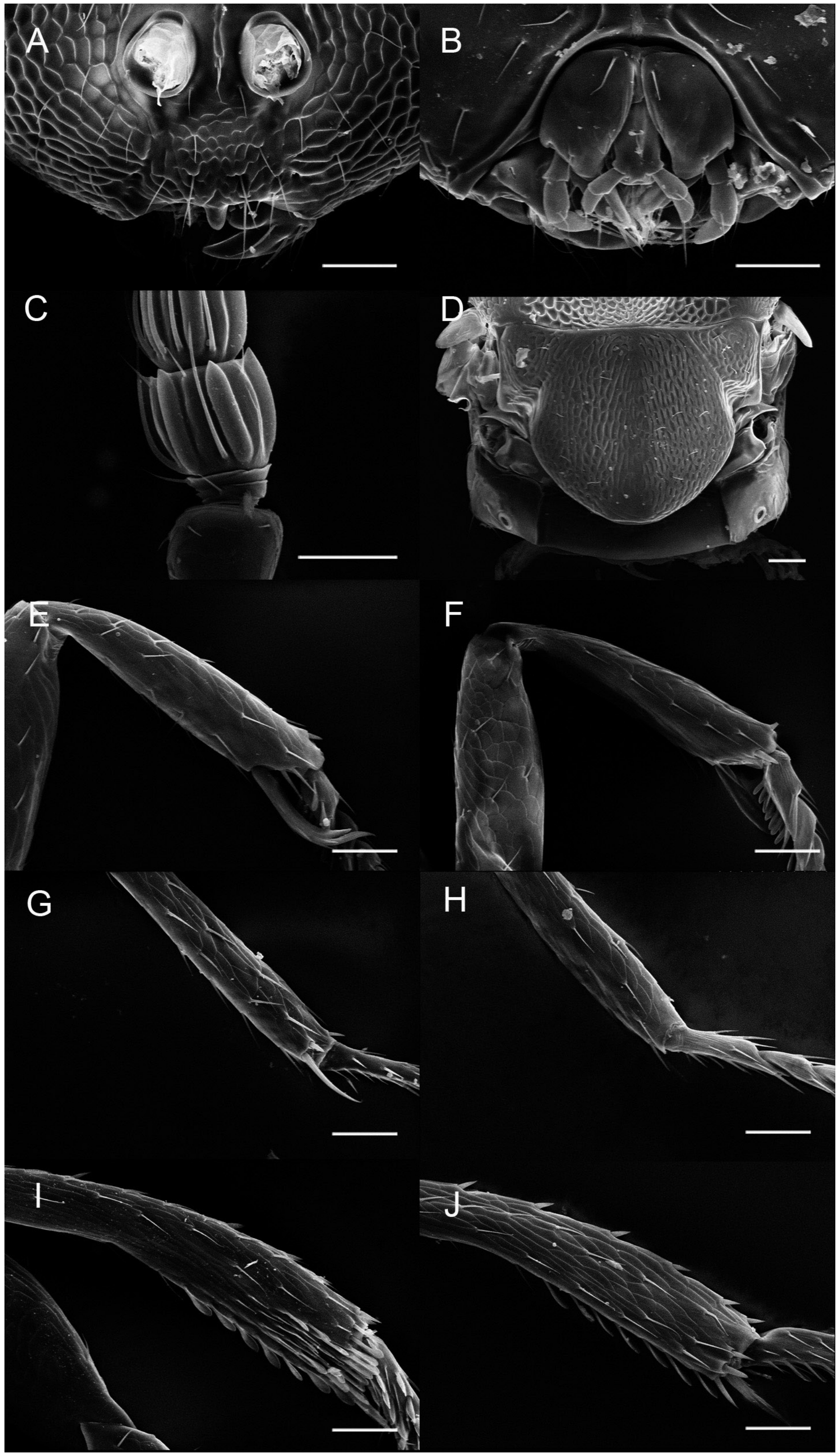

Fig. 16. Scanning electron images of female *Sycoscapter littoralis* sp. nov. A, Toruli and epistomal margin; B, Maxillary palps and labial palps; C, Anelli and the first funiculus; D, Scutellum; E, Left fore tibia, axial; F, Right tibia, antiaxial; G, Left mid tibia, axial; H, Right mid tibia, antiaxial; I, Right hind tibia, axial; J, Left hind tibia, antiaxial. Scale bar = 0.03 mm.

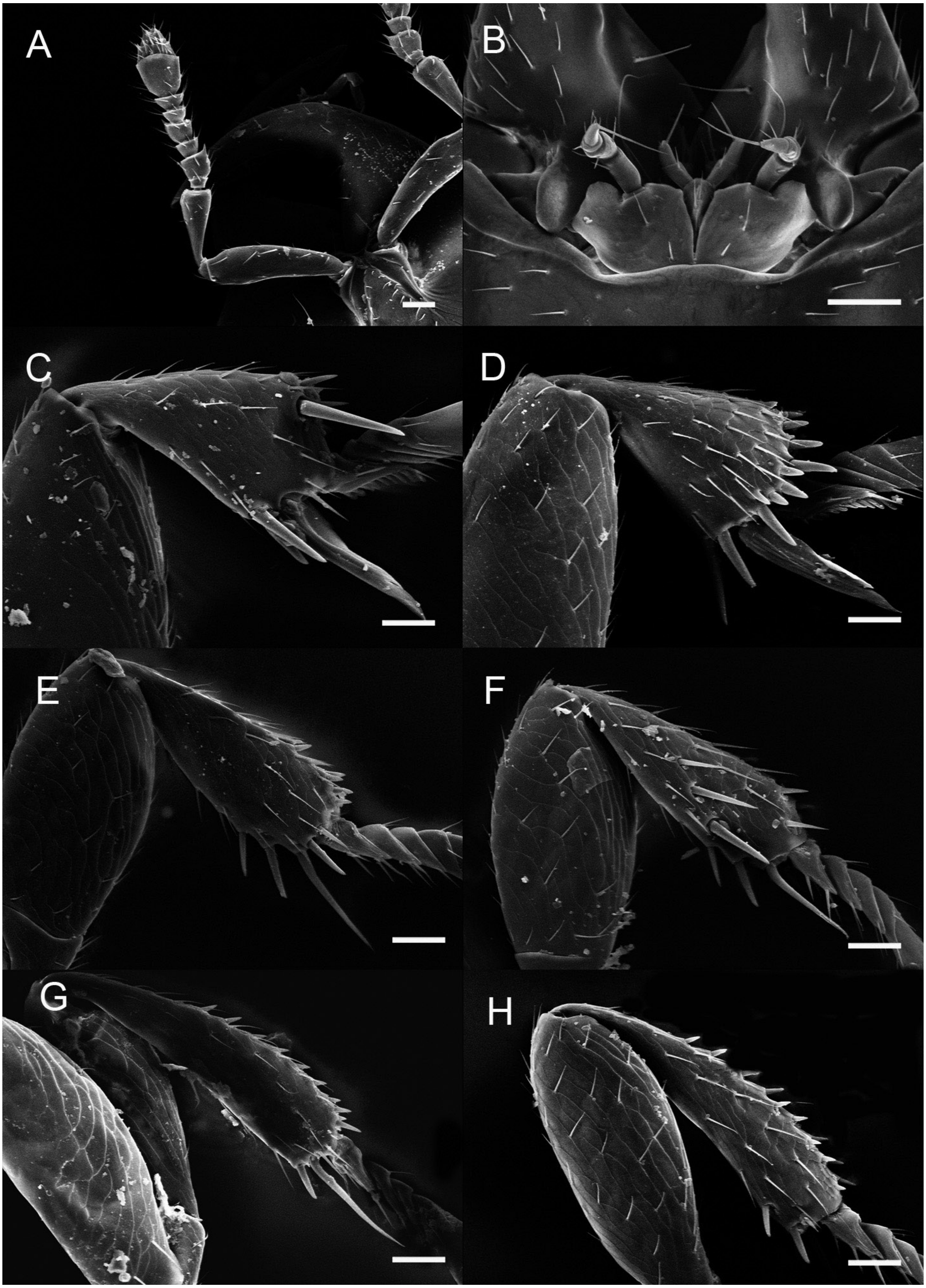

Fig. 17. Scanning electron images of male *Sycoscapter littoralis* sp. nov. A, Antenna; B, Maxillary palps and labial palps; C, Left fore tibia, axial; D, Right tibia, antiaxial; E, Left mid tibia, axial; F, Right mid tibia, antiaxial; G, Right hind tibia, axial; H, Left hind tibia, antiaxial. Scale bar = 0.03 mm.

8. Head subhexagonal (Fig. 9E); anterior margin of pronotum convex obviously (Fig. 9F) .... *S. monticola*
- Head long rectangular (Figs. 12E; 15E); anterior margin of pronotum not convex obviously (Figs. 12F; 15F) 9
9. Mesosoma subpentagonal (Fig. 12F); pronotum L 1.5× L of the fused tergum (Fig. 12F) .... *S. ishiianus*
- Mesosoma ovate (Fig. 15F); pronotum L 2× L of the fused tergum (Fig. 15F) .... *S. littoralis*

DISCUSSION

In this study, we collected all six monoecious fig species in Taiwan and documented the presence of five *Sycoscapter* wasp species associated with these figs with the exception of *F. pubinervis*, the rarest monoecious fig species in Taiwan. Notably, a previous study (Segar et al. 2012) had reported the association of one *Sycoscapter* wasp with *F. pubinervis*. The absence of this *Sycoscapter* wasp in our collection could be attributed to the limited distribution of *F. pubinervis* in Taiwan. Wang et al. (2015) documented a decline in the species richness of fig wasps associated with *F. microcarpa* along latitude or altitude, indicating that certain wasp species may struggle to colonize figs in marginal distribution areas.

Although the *COI* gene has been considered less reliable for species delimitation in fig wasps owing to rampant heteroplasmy (Xiao et al. 2010; Li et al. 2021), the phylogenetic trees based on *COI+28S* combined data and the results of PTP method exhibited a consistent trend, supporting the existence of five *Sycoscapter* species associated with monoecious figs in Taiwan. This finding was also supported by the substantial genetic gaps among all *Sycoscapter* species in this study. Moreover, aligning with the wide distribution of their host fig trees, most of these *Sycoscapter* wasps exhibited broad geographic ranges, extending from China to Taiwan or from Taiwan to the Ryukyu Islands, Japan. Although a direct observation of *Sycoscapter* wasp dispersal ability is lacking, it is reasonable to assume that they possess a wider distribution range compared with agaonid wasps, which are known to disperse up to 160 km via wind (Ahmed et al. 2009; Sutton et al. 2016).

Our findings revealed that both *S. gajimaru* and *S. piceoscapus* used *F. microcarpa* and *F. benjamina* var. *bracteata* as host species. Given the close relationship between these two *Ficus* species and their similar fig sizes during receptive and developing phases (4–7 mm in *F. microcarpa* vs. 5–7 mm in *F. benjamina* var. *bracteata*; Tzeng 2004), the transition between these two host figs appears to be relatively unrestricted, likely owing to minimal impedance from the fig wall (Fan et al. 2019). Furthermore, the use of multiple fig species by sycoryctina wasps has been observed in numerous studies (Silvieus et al. 2008; McLeish et al. 2012), suggesting that flexible host specificity is not uncommon in this wasp group.

In accordance with Bouček et al. (1981) and Pramanik and Dey (2019), several female-specific characters have been used to differentiate *Sycoscapter* species, including POL/OOL ratio, the number of setae on the forewing, the ratio of marginal vein to stigma vein L, and the ratio of ovipositor L/metasoma L. However, among these characters, the number of setae on the forewing has been reported to be highly variable (Wiebes 1967), with variations observed not only between individuals in the same population but also within the wings of the same individual. In contrast, the POL/OOL character appears to be reliable for the identification of *Sycoscapter* wasps, as it has exhibited effectiveness in not only the studied *Sycoscapter* wasps but also in other pteromalid groups (Graham 1969; Bouček and Rasplus 1991). In addition, the taxonomic value of spine or tooth number on the legs was examined in this study as it had been regarded as a character to identify species in another fig wasp genus (Ulenberg and van Pelt 1985). Our results revealed spine number on legs of males might be used as a character at the morpho-group level, but not at species level due to its variation between individuals of a species. Although several taxonomic studies have described *Sycoscapter* species based solely on females (Walker 1871; Risbec 1956), this approach can lead to taxonomic challenges, especially when species exhibit substantial sexual dimorphism (Walker 1871; Westwood 1883), as observed in the present study. Interestingly, our findings suggest that male characters may have greater taxonomic value, particularly the varied and distinct male head shapes. Despite reports of male polymorphism in fig wasps being common (Murray 1990; Bean and Cook 2001; Jousselin et al. 2005), our observations indicate polymorphism in male heads was limited to size variation among the five *Sycoscapter* species, underscoring the potential value of male head shape as a taxonomic character in this study.

Although this study focused exclusively on species associated with monoecious figs, the shared wing vestige among them does not necessarily imply that they form a monophyletic group compared with species associated with functional dioecious figs. Despite the terms ‘rudimentary wing vestige’ or ‘remnant wing’ (Westwood 1883; Wiebes 1966), it is unlikely that this structure serves as a mere vestige, given the presence of numerous fine hairs that may serve sensory functions as male individuals navigate the internal galls and seeds of a fig. The differences in internal microhabitats between monoecious and functional dioecious figs have been documented in various studies (Kerdelhué and Rasplus 1996; Weiblen 2000), with the most notable distinction being the layer structure composed of galls and seeds, which forms multiple layers in monoecious figs and a single layer in functional dioecious figs (Kerdelhué and Rasplus 1996). Similarly, the presence of the wing vestige in male wasps of the genera *Otitesella* and *Walkerella*, which belong to the pteromalid tribe Otitesellini and are primarily associated with monoecious fig trees (Jousselin et al. 2006; Ma et al. 2013), suggests that these males may have evolved similar habits or behaviors inside their native figs. Therefore, the wing vestige is more likely an adaptive convergent character rather than a synapomorphic character.

This study, including a thorough collection effort, represents the first comprehensive taxonomic assessment of *Sycoscapter* wasps associated with monoecious figs in Taiwan. Given the reported keystone status of fig species (Mackay et al. 2018), it is crucial to identify species composition in fig-wasp communities and understand their interactions within multitrophic ecosystems. Although taxonomic studies of *Sycoscapter* species associated with functional dioecious figs remain to be conducted, this study not only contributes to the knowledge of chalcidoid fauna in Taiwan but also provides insights into the mechanism underlying the maintenance of this intricate ecosystem.

CONCLUSIONS

Wasps of the genus *Sycoscapter* (Hymenoptera: Pyeromalidae) associated with monoecious *Ficus* species in Taiwan were investigated. Both phylogenetic and morphological results indicated presence of five species among those wasps, including four new species: *S. piceoscapus* sp. nov., *S. monticola* sp. nov., *S. ishiianus* sp. nov. and *S. littoralis* sp. nov. This discovery not only records new members of Taiwanese chalcid fauna but also provides insight into fig-wasp symbiosis.

Acknowledgment: We thank Ayako Sasaki, Junko Kusumi and Kouichi Arimoto for collecting samples in Japan. We also thank Chi-Feng Lee and Junsuke Yamasako for their kind help during specimen examination at Taiwan Agricultural Research Institute, Taichung, Taiwan; and Institute for Agro-Environmental Sciences, Ibaraki, Japan. We are grateful to Hengchun Research Center, Forestry Research Institute and Lanyu township office for their kind help during our field collection.

Authors' contributions: PAC and HYT conceived the ideas; WBY and HYT developed the research program; PAC, ZHS and HYT collected the data; PAC, WBY and ZHS carried out the analyses; PAC drafted the manuscript; all authors have read, edited and agreed to the published version of the manuscript.

Competing interests: The authors declare that they have no competing interests.

Availability of data and materials: All specimens are deposited in museum collections stated in the paper. All DNA sequence data has been deposited in GenBank (accession number PP111396-PP111462 and PP162908-PP162951).

Consent for publication: All authors consent to the publication of this manuscript.

Ethics approval consent to participate: No applicable.

REFERENCES

Ahmed S, Compton SG, Butlin RK, Gilmartin PM. 2009. Wind-borne insects mediate directional pollen transfer between desert fig trees 160 kilometers apart. Proc Natl Acad Sci USA **106:**20342–20347. doi:10.1073/pnas.0902213106.

Azuma H, Harrison RD, Nakamura K, Su ZH. 2010. Molecular phylogenies of figs and fig-pollinating wasps in the Ryukyu and Bonin (Ogasawara) islands, Japan. Genes and Genet Syst **85:**177–192. doi:10.1266/ggs.85.177.

Bean D, Cook JM. 2001. Male mating tactics and lethal combat in the nonpollinating fig wasp *Sycoscapter australis*. Anim Behav **62:**535–542. doi:10.1006/anbe.2001.1779.

Berg CC, Wiebes JT. 1992. African Fig Trees and Fig Wasps. Koninklijke Nederlandse Akademie van Wetenschappen Verhandelingen Afdeling Natuurkunde, Amsterdam, Netherland.

Berg CC, Corner EJH. 2005. Moraceae: Ficeae. *In*: van Welzen PC (ed) Flora Malesiana Series I (Seed Plants), Vol 17. National Herbarium Nederkand: Leiden, Netherland.

Borges RM. 2015. How to be a fig wasp parasite on the fig-fig wasp mutualism. Curr Opin Insect Sci **8:**34–40. doi:10.1016/j.cois.2015.01.011.

Bouček Z, Watsham A, Wiebes JT. 1981. The fig wasp fauna of the receptacles of *Ficus thonningii* (Hymenoptera, Chalcidoidea). Tijdschr Entomol **124:**149–233.

Bouček Z. 1988. Australian Chalcidoidea (Hymenoptera): a biosystematic revision of genera of fourteen families, with a reclassification of species. CABI, Wallingford, UK.

Bouček Z, Rasplus JY. 1991. Illustrated key to West-Palearctic genera of Pteromalidae (Hymenoptera: Chalcidoidea). INRA, Paris, France.

Burks R, Mitroiu MD, Fusu L, Heraty JM, Janšta P, Heydon S, Papilloud NDS, Peters RS, Tselikh EV, Woolley JB, van Noort S, Baur H, Cruaud A, Darling C, Haas M, Hanson P, Krogmann L, Rasplus JY. 2022. From hell's heart I stab at thee! A determined approach towards a monophyletic Pteromalidae and reclassification of Chalcidoidea (Hymenoptera). J Hymenopt Res **94:**13–88. doi:10.3897/jhr.94.94263.

Chao WC, Wu SH, Fan SW, Lin HY, Hsieh CF, Chao KJ. 2008. Distribution patterns of tree species in a lowland rainforest at Nanjen Lake, southern Taiwan. Taiwania **53:**124–133. doi:10.6165/tai.2008.53(2).124.

Chen YR, Chuang WC, Wu WJ. 1999. Chalcid wasps on *Ficus microcarpa* L. in Taiwan (Hymenoptera: Chalcidoidea). J Taiwan Mus **52:**39–79.

Cook JM, Bean D. 2006. Cryptic male dimorphism and fighting in a fig wasp. Anim Behav **71:**1095–1101. doi:10.1016/j.anbehav.2005.07.027.

Cruaud A, Jabbour-Zahab R, Genson G, Cruaud C, Couloux A, Kjellberg F, van Noort S, Rasplus J. 2010. Laying the foundations for a new classification of Agaonidae (Hymenoptera: Chalcidoidea), a multilocus phylogenetic approach. Cladistics **26:**359–387. doi:10.1111/j.1096-0031.2009.00291.x.

Cruaud A, Rønsted N, Chantarasuwan B, Chou LS, Clement WL et al. 2012. An extreme case of plant-insect codiversification: figs and fig-pollinating wasps. Syst Biol **61:**1029–1047. doi:10.1093/sysbio/sys068.

Darwell CT, Cook JM. 2017. Cryptic diversity in a fig wasp community-morphologically differentiated species are sympatric but cryptic species exhibit competitive exclusion. Mol Ecol **26:**937–950. doi:10.1111/mec.13985.

Fan KY, Bain A, Tzeng, HY, Chiang, YP, Chou LS, Kuo-Huang LL. 2019. Comparative anatomy of the fig wall (*Ficus*, Moraceae). Botany **97:**417–426. doi:10.1139/cjb-2018-0192.

Gardner E, Bruun-Lund S, Niissalo M, Chantarasuwan B, Clement WL et al. 2023. Echoes of ancient introgression punctuate stable genomic lineages in the evolution of figs. Proc Natl Acad Sci USA **120:**e2222035120. doi:10.1073/pnas.2222035120.

Graham MWR de V. 1969. The Pteromalidae of north-western Europe (Hymenoptera: Chalcidoidea). Bull Br Mus Nat Hist Entomol **16:**1–908. doi:10.5962/p.258046.

Heraty J, Hawks D. 1998. Hexamethyldisilazane - a chemical alternative for drying insects. Entomol News **109:**369–374.

Heraty J, Hawks D, Kostecki JS, Carmichael A. 2004. Phylogeny and behaviour of the Gollumiellinae, a new subfamily of the ant-parasitic Eucharitidae (Hymenoptera: Chalcidoidea). Syst Entomol **29:**544–559. doi:10.1111/j.0307-6970.2004.00267.x.

Hoang DT, Chernomor O, von Haeseler A, Minh BQ, Vinh LS. 2018. UFBoot2: Improving the Ultrafast Bootstrap Approximation. Mol Biol Evol **35:**518–522. doi:10.1093/molbev/msx281.

Ishii T. 1934. Fig chalcidoid of Japan. Kontyû **8:**84–102.

Joseph KJ. 1953. Contribution to our knowledge of fig insects (Chalcidoidea: Parasitic: Hymenoptera) from India. III. Description of three new genera and five new species of Sycophagini, with notes on biology, distribution and evolution. Agra Univ J Res: Sci **2:**53–81.

Joseph KJ. 1961. Contribution to our knowledge of fig insects (Chalcidoidea: Parasitic: Hymenoptera) from India. VIII. Notes on some new fig insects. J Karnataka Univ **4:**88–100.

Jousselin E, van Noort S, Greeff JM. 2005. Labile male morphology and intraspecific male polymorphism in the *Philotrypesis* fig wasps. Mol Phylogenet Evol **33:**706–718. doi:10.1016/j.ympev.2004.08.008.

Jousselin E, van Noort S, Rasplus JY, Greeff JM. 2006. Patterns of diversification of Afrotropical *Otiteselline* fig wasps: phylogenetic study reveals a double radiation across host figs and conservatism of host association. J Evol Biol **19:**253–266. doi:10.1111/j.1420-9101.2005.00968.x.

Karube H, Kishimoto T, Mori H, Kubota M. 2022. Insect Fauna of the Iwo Islands – Characteristics of Each Island and Comparison with the Ogasawara Island Group. Res Rep Kanagawa prefect Mus Nat Hist **17:**29–54.

Kerdelhué C, Rasplus JY. 1996. The evolution of dioecy among *Ficus* (Moraceae): an alternative hypothesis involving non-pollinating fig wasp pressure on the fig-pollinator mutualism. Oikos **77:**163–166. doi:10.2307/3545597.

Lanfear R, Calcott B, Ho SYW, Guindon S. 2012. PartitionFinder: combined selection of partitioning schemes and substitution models for phylogenetic analyses. Mol Biol Evol **29:**1695–1701. doi:10.1093/molbev/mss020.

Li TC, Wang YK, Sui ZX, Wang T, Nian JZ, Jiang JZ, Tang T, Liu FS, Xiao JH, Huang DW. 2021. Multiple mitochondrial haplotypes within individual specimens may interfere with species identification and biodiversity estimation by DNA barcoding and metabarcoding in fig wasps. Syst Entomol **46:**887–899. doi:10.1111/syen.12500.

Lopez-Vaamonde C, Wikström N, Kjer KM, Weiblen GD, Rasplus J, Machado CA, Cook JM. 2009. Molecular dating and biogeography of fig-pollinating wasps. Mol Phylogenet Evol **52:**715–726. doi:10.1016/j.ympev.2009.05.028.

Ma YC, Peng YQ, Yang DR. 2013. Description of two new species of *Walkerella* (Pteromalidae, Otitesellinae) from China with a key to species of the genus. Zootaxa **3702:**473–483. doi:10.11646/zootaxa.3702.5.6.

Mackay KD, Gross GL, Rosseto M. 2018. Small populations of fig trees offer a keystone food resource and conservation benefits for declining insectivorous birds. Glob Ecol Conserv **14:**e00403. doi:10.1016/j.gecco.2018.e00403.

McLeish MJ, van Noort S, Tolley KA. 2010. African parasitoid fig wasp diversification is a function of *Ficus* species ranges. Mol Phylogenet Evol **57:**122–134. doi:10.1016/j.ympev.2010.05.025.

McLeish MJ, Beukman G, van Noort S, Wossler TC. 2012. Host-plant species conservatism and ecology of a parasitoid fig Wasp genus (Chalcidoidea; Sycoryctinae; *Arachonia*). PLoS ONE **7:**44804. doi:10.1371/journal.pone.0044804.

Murray MG. 1990. Comparative morphology and mate competition of flightless male fig wasps. Anim Behav **39:**434–443. doi:10.1016/S0003-3472(05)80406-3.

Nguyen LT, Schmidt HA, von Haeseler A, Minh BQ. 2015. IQ-TREE: a fast and effective stochastic algorithm for estimating maximum-likelihood phylogenies. Mol Biol Evol **32:**268–274. doi:10.1093/molbev/msu300.

Pramanik A, Dey D. 2019. Two new fig wasp species of genus *Sycoscapter* Saunders, 1883 (Hymenoptera: Chalcidoidea: Pteromalidae) with a key to species of the genus from India. Taiwania **64:**139–148. doi:10.6165/tai.2019.64.139.

Priyadarsanan DR. 2000. Fig insects of Kerala. Rec of the Zool Surv India **182:**1–175.

Rambaut A, Drummond AJ, Xie D, Baele G, Suchard MA. 2018. Posterior summarisation in Bayesian phylogenetics using Tracer 1.7. Syst Biol **67:**901–904. doi:10.1093/sysbio/syy032.

Risbec J. 1956. Torymidae et Agaonidae de Madagascar (Hym. Chalcidoidea). Annu Soc Entomol Fr **124:**149–194.

Ronquist F, Teslenko M, van der Mark P, Ayres DL, Darling A, Höhna S, Larget B, Liu L, Suchard MA, Huelsenbeck JP. 2012. MrBayes 3.2: efficient Bayesian phylogenetic inference and model choice across a large model space. Syst Biol **61:**539–542. doi:10.1093/sysbio/sys029.

Segar ST, Lopez-Vaamonde C, Rasplus JY, Cook JM. 2012. The global phylogeny of the subfamily Sycoryctinae (Pteromalidae): parasites of an obligate mutualism. Mol Phylogenet Evol **65:**116–125. doi:10.1016/j.ympev.2012.05.030.

Silvieus SI, Clement WL, Weiblen GD. 2008. Cophylogeny of figs, polliantors, gallers and parasitoids. *In*: Tilmon K (ed).

Specialization, Speciation and Radiation: The Evolutionary Biology of Herbivorous Insects. University of California Press, California, USA.
Sutton TL, Riegler M, Cook JM. 2016. One step ahead: a parasitoid disperses farther and forms a wider geographic population than its fig wasp host. Mol Ecol **25:**882–894. doi:10.1111/mec.13445.
Tamura K, Stecher G, Kumar S. 2021. MEGA11: Molecular Evolutionary Genetics Analysis Version 11. Mol Biol Evol **38:**3022–3027. doi:10.1093/molbev/msab120.
Tan Z, Fu Y, Sharma G, Mathews DH. 2017. TurboFold II: RNA structural alignment and secondary structure prediction informed by multiple homologs. Nucleic Acids Res **45:**11570–11581. doi:10.1093/nar/gkx815.
Trifinopoulos J, Nguyen LT, von Haeseler A, Minh BQ. 2016. W-IQ-TREE: a fast online phylogenetic tool for maximum likelihood analysis. Nucleic Acids Res **44:**W232–W235. doi:10.1093/nar/gkw256.
Tzeng HY. 2004. Taxonomic study of the genus *Ficus* in Taiwan. PhD dissertation. National Chung-Hsin University, Taichung, Taiwan.
Tzeng HY, Ou CH, Lu FY, Bain A, Chou LS, Kjellberg F. 2014. The effect of fig wall thickness in *Ficus erecta* var. *beecheyana* on parasitism. Acta Oecol **57:**38–43. doi:10.1016/j.actao.2013.06.007.
Ulenberg SA, van Pelt W. 1985. A revision of the species of Apocrypta Coquerel: a taxonomic study incorporating uni- and multivariate analyses. Verh Kon Ned Akad Wetensch **83:**41–148.
van Noort S, Rasplus JY. 2024. Figweb: figs and fig wasps of the world. Available at: www.figweb.org. (Accessed on 29 Apr. 2024).
Walker F. 1871. Part IV. Chalcididae, Leucospidae, Agaonidae, Perilampidae, Ormyridae, Encyrtidae. In: Notes on Chalcidiae, Janson EW, London, UK.
Walther BA, Geier J, Chou LS, Bain A. 2018. The figs of winter: Seasonal importance of fruiting fig trees (*Ficus*: Moraceae) for urban birds. Acta Oecol **90:**28–34. doi:10.1016/j.actao.2017.11.015.
Wang R, Compton SG, Quinnell RJ, Peng YQ, Baewell L, Chen Y. 2015. Insect responses to host plant provision beyond natural boundaries: latitudinal and altitudinal variation in a Chinese fig wasp community. Ecol Evol **5:**3642–3656. doi:10.1002/ece3.1622.
Weiblen GD. 2000. Phylogenetic relationships of functionally dioecious *Ficus* (Moraceae) based on ribosomal DNA sequences and morphology. Am J Bot **87:**1342–1357. doi:10.2307/2656726.
Weiblen GD. 2002. How to be a fig wasp. Annu Rev Entomol **47:**299–330. doi:10.1146/annurev.ento.47.091201.145213.
Westwood JO. 1883. Further descriptions of insects infesting figs. Trans R Entomol Soc Lond **31:**29–47. doi:10.1111/j.1365-2311.1883.tb02938.x.
Wiebes JT. 1966. Bornean fig wasps from *Ficus stupenda* Miquel (Hymenoptera, Chalcidoidea). Tijdschr Entomol **109:**163–192.
Wiebes JT. 1967. Redescription of Sycophaginae from Ceylon and India, with a designation of lectotypes, and a world catalogue of the Otitesellini (Hymenoptera Chalcidoidea Torymidae). Tijdschr Entomol **110:**399–442.
Xiao JH, Wang NX, Li YW, Murphy RW, Wan DG, Niu LM, Hu HY, Fu YG, Huang DW. 2010. Molecular approaches to identify cryptic species and polymorphic species within a complex community of fig wasps. PLoS ONE **5:**e15067. doi:10.1371/journal.pone.0015067.
Yang LY, Machado CA, Dang XD, Peng YQ, Yang DR, Zhang DY, Liao WJ. 2014. The incidence and pattern of copollinator diversification in dioecious and monoecious figs. Evolution **69:**294–304. doi:10.1111/evo.12584.
Yokohama J, Iwatsuki K. 1998. A faunal survey of fig-wasps (Chalcidoidea: Hymenoptera) distributed in Japan and their associations with figs (Ficus: Moraceae). Entomol Sci **1:**37–46.
Zhang JJ, Kapli P, Pavlidis P, Stamatakis K. 2013. A general species delimitation method with applications to phylogenetic placements. Bioinform **29:**2869–2976. doi:10.1093/bioinformatics/btt499.

Supplementary materials

Table S1. Monoecious *Ficus* species in Taiwan and their distributions according to Flora of Taiwan Vol. 2 (2nd edition). (download)

Fig. S1. Phylogenetic tree of the *Sycoscapter* species associated with monoecious figs in Taiwan and other congeners based on *28S* genes. The values at the nodes are the ultrafast bootstraps and posterior possibilities for maximum likelihood (ML) and Bayesian inference (BI) analyses, respectively. (download)

Fig. S2. Lectotype of *Sycoscapter gajimaru* (Ishii). A, female specimen; B, label. (download)